Functional assessment of 3'UTR regulatory elements using the zebrafish (*Danio rerio*) model system - towards modulating protein levels in Atlantic salmon (*Salmo salar*) for more sustainable aquaculture

Morten Barvik

Master thesis, Molecular Biology. Department of Biological Sciences (BIO), University of Bergen.

November 2021

Abstract

Post-transcriptional regulation is a complex process that encompasses a myriad of different structures and mechanisms. There are several indications that regulatory elements in the 3'UTR play an important role in the stability of mRNA transcripts. Sequences of 60 nucleotide base pairs from the 3'UTR of two genes, *trip10a* from zebrafish and *mx2.2* from Atlantic salmon, were identified to contain Adenylate-uridylate-rich elements (AU-rich elements; AREs). AREs are proposed to have a destabilizing effect on mRNA stability. We mutated the identified AREs, and inserted both unmutated wild type (WT) and mutated 60 bp sequence elements into the 3'UTR of a GFP expression construct. Zebrafish embryos were subjected to two different injection experiments. In the first experiment embryos were injected with GFP mRNA containing WT and mutated 3'UTR elements from the *trip10a* gene. In the second experiment embryos were injected with GFP mRNA containing WT and two different mutated versions of 3'UTR elements from the *mx2.2* gene. Zebrafish embryos were injected at the 1-cell stage and measured for fluorescence intensity at 6, 12, 24, 48, 72, 96, and 120 hpf. GFP Fluorescence was normalized by injecting embryos with 75 ng/µL mCherry RFP mRNA and mRNA stability was assessed by detection of GFP and RFP fluorescence signals. The mutated *trip10a* 3'UTR caused a significant increase in GFP levels ($p < 0.01$). Mutations in two AREs (Mutation A) from the *mx2.2* 3'UTR caused a significant increase in GFP levels ($p < 0.05$). Mutations in two AREs and a selection of AT repeats (Mutation B) caused a significant increase in GFP levels ($p < 0.05$). These results support the approach in this thesis as a robust method for using zebrafish as a model to assess mRNA stability. This method can be used to test and assess putative regulatory elements for mRNA stability in salmon, and subsequently used to modulate expression of key anti-viral proteins to make salmon more robust against disease. This can thus be a small step towards a more sustainable salmon aquaculture.

Acknowledgements

The work presented in this thesis was conducted at the University in Bergen (UiB) and Institute of Marine Research (IMR). This thesis was a part of the project; TUNESAL-Robust Atlantic salmon through fine-tuned genome editing.

First and foremost, I would like to sincerely thank my supervisors Ståle Ellingsen at UiB and Rolf Brudvik Edvardsen at IMR for the support and guidance throughout this period of working in the lab and writing my master thesis. Thank you for your patience and interest in the work that I have done. You have always been within easy reach to answer a question or five, and I appreciate that.

I would like to express my sincere gratitude to Mari Raudstein, for the invaluable help she provided during the lab-work and countless discussions we had during the work on this thesis. You have been an inspiration and I truly value all the conversations we had. I would also like to thank Elsa Denker for teaching me techniques and helping out whenever I needed assistance in the lab. Whatever the issue was, big or small, you always took the time to show me how to solve it. A thank you goes out to Dorothy Jane Dankel, for monthly discussions about the topic of conducting proper ethical research. The discussions with you were always interesting, educational and enjoyable.

I would also like to thank my family, friends and fellow students for supporting me during this year. Finally, a special thanks goes out to Karoline, my partner in life, for always supporting and believing in me.

Bergen, November 2021
Morten Barvik

Contents

List of Figures

List of Tables

Abbreviations

ARE	**A**U-**R**ich **E**lement
ASRV	**A**tlantic **S**almon **R**eo**V**irus
BIO	Department of **BIO**logical Sciences
bp	**b**ase **p**air
BSA	**B**ovine **S**erum **A**lbumin
Cas9	**C**RISPR **as**sociated protein 9
CRISPR	**C**lustered **R**egulatory **I**nterspaced **S**hort **P**alindromic **R**epeats
DNA	**D**eoxyribo**N**ucleic **A**cid
GFP	**G**reen **F**luorescent **P**rotein
HDR	**H**omology **D**irected **R**epair
hpf	**h**ours-**p**ost **f**ertilization
IMR	The **I**nstitute of **M**arine **R**esearch
IPVN	**I**nfectious **P**ancreatic **N**ecrosis **V**irus
ISAV	**I**nfectious **S**almon **A**nemia **V**irus
LB	**L**Luria-**B**ertani
mRNA	**m**essenger **R**ibo**N**ucleic **A**cid
MZT	**M**aternal-**Z**ygotic **T**ransition
NCBI	**N**ational **C**enter for **B**iotechnology **I**nformation
NEB	**N**ew **E**ngland **B**iolabs
PD	**P**ancreas **D**isease
PEV	**P**osition **E**ffect **V**ariegation

PMCV	**P**iscine **M**yo**C**arditis **V**irus
qPCR	**q**uantitative **P**oly **C**hain **R**eaction
RBP	**R**NA-**B**inding **P**rotein
RFP	**R**ed **F**luorescent **P**rotein
RNA	**R**ibo**N**ucleic **A**cid
SAV	**S**almonid **A**lpha**V**irus
SOC	**S**uper-**O**ptimal broth with **C**atabolite repression
SWT	**S**potty **W**ild **T**ype
TAE buffer	**T**ris-**A**cetate **E**DTA buffer
TE buffer	**T**ris **E**DTA buffer
UiB	**U**niversity **i**n **B**ergen
UTR	**U**n**T**ranslated **R**egion
WT	**W**ild **T**ype

Introduction

1.1 Post-transcriptional regulation

Post-transcriptional regulation has a major influence on spatial, temporal and the level of gene expression in an organism. There are theories suggesting that the origin of multicellular life can be traced back to evolutionary changes in how organisms regulate gene expression [1]. Although all cells in an organism share the same genetic material, different cells with differing specialized functions are generated. This is due to tightly controlled regulatory mechanisms which enable differential gene expression in multicellular organisms. Regulation of gene expression occurs at several levels, including transcription, post-transcription, translation and post-translation.

Transcription occurs in the cell nucleus, where unpacking of chromatin exposes regions of DNA to enable initiation of gene transcription. Various mechanisms either repress or activate certain regions of DNA during this process as a means of early regulation of gene expression [2]. Transcription of a gene starts at the promoter, a sequence of nucleotides in the DNA recognized by RNA polymerase. RNA polymerase binds to the promoter and transcribes the gene downstream until it reaches a transcription termination region, a sequence of DNA which prompts RNA polymerase to stop the transcription. Sequences termed enhancers, which bind transcription factors that have a strong influence on gene expression [3], can enhance the expression of a certain gene. The initial product of gene

transcription is the primary transcript (pre-mRNA) which contains both introns and exons (Figure 1.1).

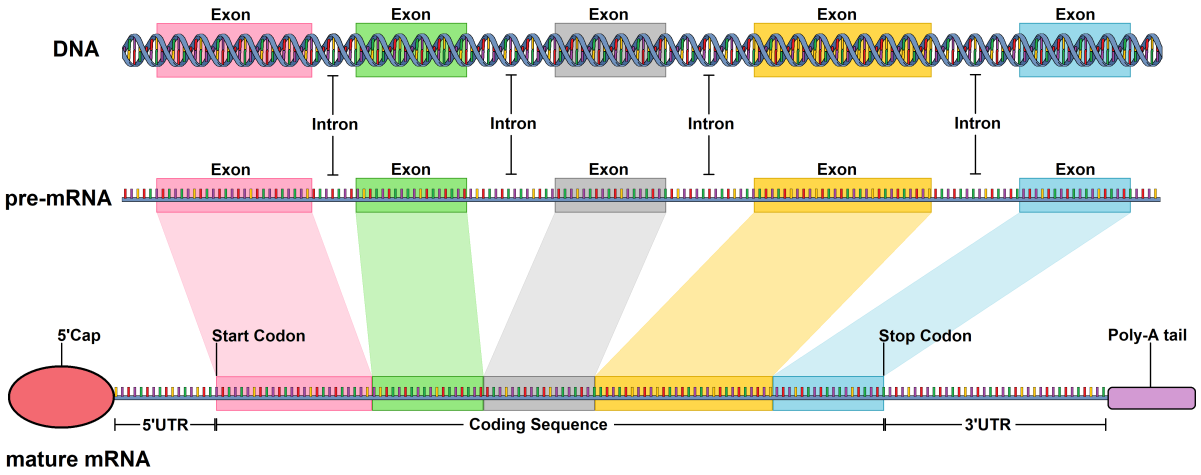

FIGURE 1.1: Overview of transcription. DNA containing exons and introns are transcribed into pre-mRNA before splicing occurs and removes the introns. The final mature mRNA transcript containing 5'cap, 5'UTR, the coding sequence, 3'UTR, and the Poly-A tail.

The pre-mRNA undergoes splicing, which removes the introns from the pre-mRNA and stitches together the remaining exons. Alternative splicing can lead to the final mature mRNA including various combinations of the exons found in the gene called variably spliced mRNAs, where some exons have been excluded in certain variants of the mRNA. This splicing process is the reason that one gene can produce proteins that differ slightly in their amino acid composition, termed protein isoforms. It is predicted that about 95 % of all human genes undergo alternative splicing processes [4].

In early embryonic development, two different sets of mature mRNA transcripts from different origins are present in the organism, maternal mRNA and zygotic mRNA [5]. Maternal mRNA is deposited into the egg by the mother. At a point during embryonic development maternal mRNA is being degraded. Simultaneously, transcription of zygotic mRNA increases rapidly. This is called the maternal-zygotic transition (MZT) [6]. There is evidence that the degradation of maternal mRNA pre-MZT is mostly a function of microRNAs, in particular miR-430 in zebrafish (*Danio rerio*) [7]. In zebrafish, zygotic

transcription starts at about 3 hours post fertilization (hpf) [8], meaning that the first 3 hours of zebrafish life its genome is mostly transcriptionally silent [9].

At some point during its lifetime, a zygotic mRNA molecule will degrade and thus stop translating more protein. The half-life of a mature mRNA molecule in the cytosol is a measure of how long it takes before 50 % of the initial mRNA concentration has degraded. Bacterial mRNA exhibit short half-lives, the median half-life of *e.coli* mRNA being 3 minutes [10]. The stability of mammalian mRNA, however, is in general considerably longer, ranging from a couple of minutes to more than 24 hours [11], with a median half-life of 10 hours in humans [12]. The longer it takes for the mRNA to decay more mRNA is present in the cytosol and potentially more protein can be translated. The stability of mRNA is highly influenced by the untranslated regions (UTR) of the mRNA transcript. Recent studies show that the 5'UTR might be an interesting topic for mRNA stability [13]. However, most studies have been primarily focused on the 3'UTR [14].

1.1.1 Regulatory elements in mRNA 3'UTR

The untranslated regions of mRNA, 5'UTR and 3'UTR, make up the regions of an mRNA transcript which is not translated into a protein. The 5'UTR is the region found upstream of the start codon, while the 3'UTR is located downstream of the stop codon. The 3'UTR has been linked to mRNA stability, and specific sequences found in the 3'UTR of mRNA suggest that certain combinations of nucleotides are directly involved in mRNA degradation in humans [15] and in zebrafish [16, 17]. Three of these sequences, AUUA, AUUUA and AAAUAAA, has been proposed to be de-stabilizing elements in the 3'UTR [16]. These three elements belong to a group of regulatory elements called Adenylate-uridylate-rich elements (AU-rich elements; AREs). AREs are regions in the mRNA 3'UTR containing a high density of A and U residues [18]. The effect of ARE in the 3'UTR on mRNA stability has been studied extensively [19, 20]. Other notable regulatory elements in the 3'UTR of mRNA are the length of the poly-A tail [21] and microRNA target sites [22].

1.2 Atlantic salmon aquaculture

Salmon farming constitutes a major part of Norwegian exports. Norway is the largest producer of Atlantic salmon (*Salmo salar*) in the world, with more than 1.3 million tonnes in 2019 [23]. A further expansion of the industry is hampered by sustainability and welfare issues. The largest and most severe of these issues is the prevalence of Salmon lice [24]. Other issues are escapees from aquaculture farms mingling with the wild Salmon population, different feeds used in aquaculture, and last but not least viral and bacterial diseases. The annual fish health report by the Norwegian veterinary institute [25] provides an overview of fish health within Norwegian aquaculture. The report provides statistics on the frequency of reported cases of various diseases ranging from viral infections, bacterial diseases, fungal diseases and parasites. SAV (Salmonid AlphaVirus) is a virus that causes pancreas disease (PD) in marine salmon farms. Reported cases for PD in Norway have almost doubled in the last decade [25]. SAV has several different genotypes and two of these genotypes, SAV2 and SAV3, have been reported in Norway. SAV3 was first reported in 2003-04 in the western regions of Norway, while SAV2 has been reported in the middle of Norway since 2010.

In many animals, including salmon, Mx proteins play a major role in the innate cellular protection against viruses. In salmon a number of viruses including IPVN [26], ASRV [27], PMCV [28], ISAV [26] and SAV [29] have been shown to induce Mx. The recent salmon genome duplication gave rise to the two clusters of Mx genes on chromosome 12 and on chromosome 25. A study of the genetic differences between salmon populations in Norway found significant differences between populations on chromosome 25 [30]. A hypothesis is that the cluster on chromosome 12 has kept more of an ancestral general function, and that genes clustered on chromosome 25 may have sub-functionalized into a more specialized defense against certain types or strains of virus [30]. To further investigate this in the TUNESAL project, ongoing project at the Institute of Marine Research (IMR) of which this thesis is a part of, CRISPR/Cas9 knock-out of an mx gene (*mx2.2*) on chromosome 25 has been carried out (unpublished results). Disease challenge studies in

the TUNESAL project show that the *mx2.2* crispants had increased the susceptibility to SAV3. This indicates that perhaps an increase in expression of this gene may lead to increased resistance to the virus. A way this can be obtained is to modify the 3'UTR in salmon using CRISPR/Cas9 mediated homology directed repair (HDR) [31, 32]. But, in order to do so one would need a method to investigate which elements influence RNA stability in salmon.

1.3 Zebrafish as a model organism

Zebrafish is a member of the minnow family (*Cyprinidae*) and has been widely utilized as a model organism for genetics, developmental biology and bio-medicine for the last four decades [33]. Zebrafish eggs are small, about 1 mm in diameter, and with adult zebrafish rarely exceeding 5 cm in length, they do not take up much space and thus are cheap and easy to maintain. Zebrafish in the wild will mate seasonally, however domesticated zebrafish in the laboratory will mate on a circadian cycle [34]. Depending on the breeding conditions, zebrafish can lay about 200-500 eggs once every week. Zebrafish is a vertebrate, making it distinct from other commonly used model organisms such as the transparent nematode worm (*Caenorhabditis elegans*) and the fruit fly (*Drosophilia Melanogaster*). Rat (*rattus norvegicus*) and mouse (*mus musculus*) are other common vertebrate model organisms used in biological studies, however, zebrafish possess qualities that makes it an ideal complementary model. Beneficial properties of zebrafish are their ex-utero development and transparent development. Thus, it is possible to observe biological processes in real time throughout embryo development, and fluorescent expression systems, e.g. GFP, can be easily applied and analysed by in vivo imaging. In addition to this, zebrafish embryos develop rapidly. Already at 24 hpf the zebrafish embryo has a heartbeat [35] and most major organs are visible. The embryo hatches between 48-72 hpf and after hatching the zebrafish embryo is now termed a zebrafish larva.

The entire zebrafish genome has been sequenced by the Wellcome Trust Sanger Institute. Zebrafish has been used extensively as a model for studying human disease [36–40]. The genome of the Zebrafish is estimated to have about 1.67 Gb spread out over 25 pairs of chromosomes. According to the National Center for Biotechnology Information (NCBI), about 30000 protein-coding genes can be found in the zebrafish genome. Zebrafish underwent a whole genome duplication event in its evolutionary history [41] and approximately 70 % of all human genes have a zebrafish orthologue [42].

1.4 Zebrafish as a model for aquaculture species (Atlantic Salmon)

Atlantic salmon is an important species for aquaculture, but a number of challenges need to be solved to make the industry more sustainable [24], e.g., salmon lice, aquaculture escapees, viral and bacterial diseases, and sustainable feed. Much research remains in order to accomplish this, but the use of salmon in experimental setups has disadvantages; a long generation time (1-3 years for males and 4 years for females), slow development (3 months until hatching), and its surrounding infrastructure is costly and extensive. Zebrafish can therefore also be a good model for basic research in Atlantic salmon. It should be noted that salmon have undergone a salmonide specific whole genome duplication [43] and will for many genes have even more copies (paralogues) than zebrafish. However, zebrafish has in some cases been shown to be well suited as a model organism for Atlantic salmon [44].

1.5 Aims of the study

Modern aquaculture faces multiple challenges in order to become more economically profitable and ecologically sustainable. These challenges include escapee fish mingling with

the wild population, infectious bacterial and viral diseases, parasitic infections in the form of salmon lice, and challenges in sustainable feed for the salmonids. New promising biotechnological tools have the potential to solve some, if not all of these challenges. This thesis focuses on the preliminary stages of creating a more robust salmon with a higher resistance against viral disease. By increasing the stability of mRNA coding for proteins involved in salmon immunity, it is possible to extend the half-life of these mRNA transcripts, and in turn increase transcriptional expression of important antiviral proteins. To that end the primary aim of this thesis is:

- Develop a method for assessing the functional role of mRNA 3'UTR regulatory elements using zebrafish as a model system.

The ultimate goal of the TUNESAL project is to assess regulatory elements in salmon. Therefore the secondary aim of this thesis is:

- Disrupt 3'UTR residing regulatory elements in a key anti-viral gene in Atlantic salmon through mutations and assess whether or not the disruption of these elements has an effect on mRNA stability.

Materials and Methods

2.1 Experimental design

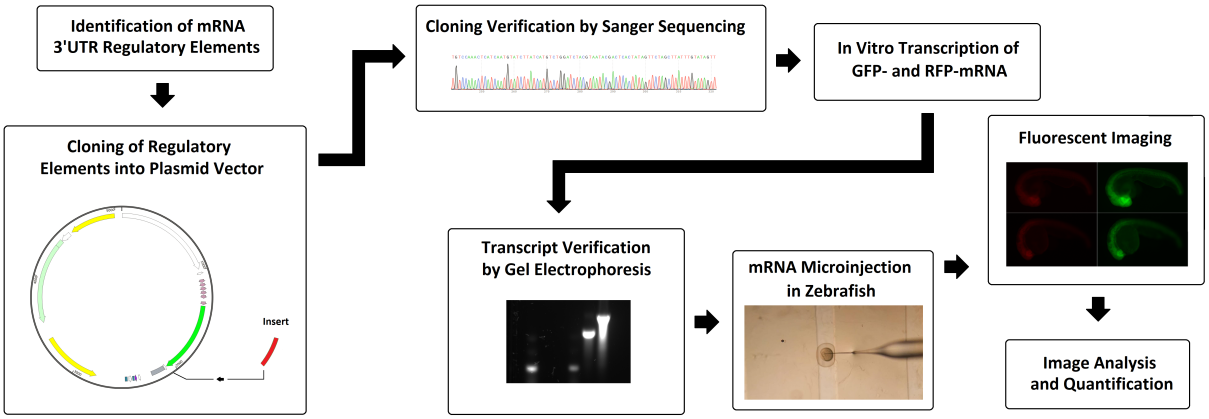

FIGURE 2.1: Overview over the experimental process used in this thesis to assess mRNA stability.

2.2 Plasmid vectors

Three different potential plasmid vectors for GFP (Green Fluorescent Protein) were tested; pCS2 mt-GFP (BamHI minus)(Addgene, USA), pUCIDT (Gift from Dr. Rabani, The Hebrew University of Jerusalem, Israel) and the pT3TS_Transposase/pDestTol2pA2_ubiEGFP system (Addgene, USA) (Figure 2.2). pCS2+8CmCherry(Addgene, USA) was used for

normalization of GFP. For ease of reading the names of the plasmids, they will be abbreviated in this thesis according to table 2.1.

TABLE 2.1: Names of plasmids used in the thesis, their abbreviation, and origin.

Plasmid	Abbreviation	Ref.
pCS2 mt-GFP (BamHI minus)	pCS2 GFP	Addgene ID:15681
pCS2+8CmCherry	pCS2 mCherry	Addgene ID:34935
pDestTol2pA2_ubiEGFP	pDestTol2	Addgene ID:27323
pT3TS_Transposase	pTransposase	Addgene ID:109768
pUCIDT	pUCIDT	[17]

2.3 Amplification of plasmids

2.3.1 LB medium and LB agar plates

Luria-Bertani (LB) agar and liquid medium was prepared for work with bacterial cultures. 1L of liquid medium and 500 mL of agar was made according to table 2.2. 500 mL agar was just enough to fill 20 Petri dishes with agar.

TABLE 2.2: LB Liquid Medium and LB agar plates reagents.

	Liquid medium	Agar
MilliQ water	950 mL	500 mL
Tryptone	10 g	5 g
NaCl	10 g	5 g
Yeast extract	5 g	2.5 g
Agar	-	7,5 g
Ampicillin	50 μg/mL*	50 μg/mL

* Ampicillin was added to the liquid medium stock prior to bacterial inoculation.

After mixing the reagents together, both solutions were autoclaved at 121 37°C for 30 minutes. After autoclaving, the mixtures was cooled down. The mixture with agar was cooled down to 37°C using spring water, and ampicillin was added. When the mixture was cool enough, it was used to coat 20 Petri dishes with about a 0.5 - 1 cm layer of agar.

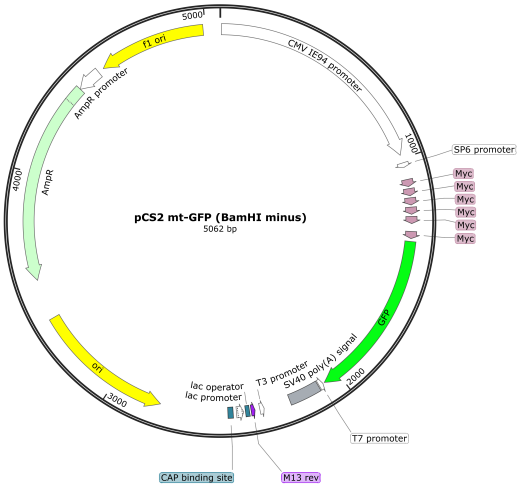

(a) pCS2 GFP

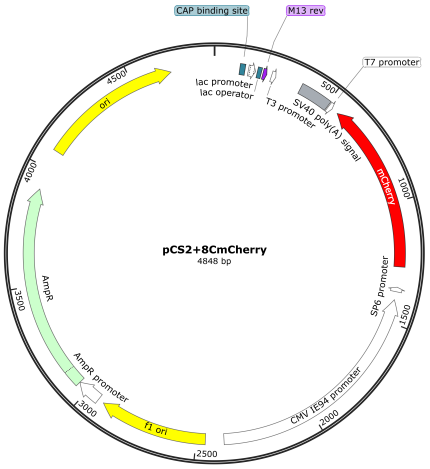

(b) pCS2 mCherry

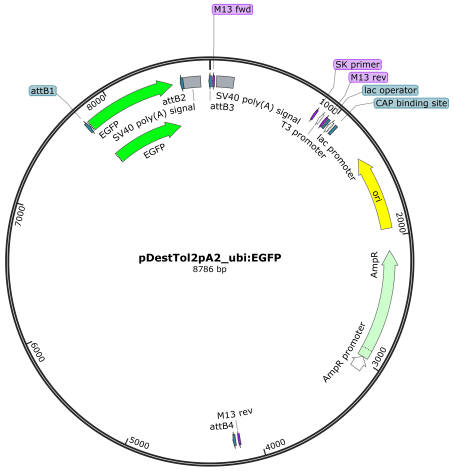

(c) pDestTol2

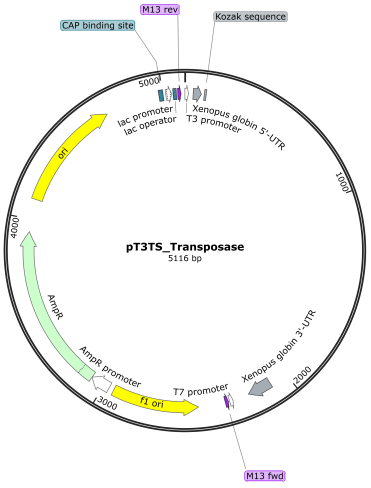

(d) pTransposase

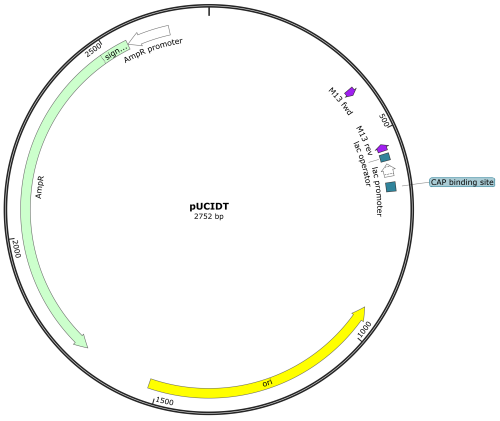

(e) pUCIDT

FIGURE 2.2: Overview over plasmids.

2.3.2 Transformation

Prior to transformation LB agar plates with ampicillin were pre-warmed in an incubator at 37°C. TOPO10 competent *E.coli* cells were thawed on ice for about 30 minutes prior to transformation. Plasmids were added to the TOPO10 cells when they had thawed and the cells were incubated on ice for 30 minutes. Cells were subjected to a heat shock in a water bath at 42°C for 30 seconds, then immediately put back on ice for 2 minutes. 750 µL of SOC-medium were added to the bacterial cells and they were incubated at 37 °C for 60 minutes. Bacteria were then plated onto ampicillin LB agar plates and left overnight. Single colonies from each Petri dish were transferred into a tube containing about 3-4 mL of liquid medium, with added ampicillin. Tubes of the liquid bacterial cultures were incubated overnight in a stirring incubator at 37°C while being stirred at 250 rpm.

2.3.3 Plasmid DNA isolation

The pUCIDT plasmid was recovered from filter paper by resuspension in 0.1x TE buffer and transformed into TOPO10 competent cells by heat shock in a water bath at 42°C for 30 seconds, then immediately put back on ice for 2 minutes. 750 µL of SOC-medium were added to the bacterial cells and they were incubated at 37°C for 60 minutes. Bacteria were then plated onto ampicillin LB agar plates and left overnight, and single colonies were inoculated in liquid medium overnight at 37°C, 250 rpm. The plasmids pCS2 GFP, pCS2 mCerry and pTransposase were inoculated from agar stabs by using an inoculation loop to transfer bacteria to an agar plate. Single colonies from the plate were inoculated in liquid medium overnight at 37°C, 250 rpm.

Plasmid DNA was isolated from bacterial pellets from overnight liquid bacterial cultures using QIAprep® Spin Miniprep Kit (Qiagen, USA) as described by the manufacturer. Briefly, 2 mL of bacterial culture were pelleted in a 2 mL eppendorf tube by centrifugation at 8000 rpm for 3 minutes and resuspended in 250 µL buffer P1. 250 µL of buffer P2 was added and the solution was inverted 6 times and set to incubate for a couple of minutes,

making sure the incubation time would not exceed 5 minutes. 350 µL Buffer N3 was added and the solution was immediately inverted 6 times. The solution was centrifuged for 10 minutes at 13.000 rpm. 800 µL of the resulting supernatant was transferred to a spin column. The spin column was centrifuged for 45 seconds at 13.000 rpm and the flow through was discarded. The spin column was washed with 500 µL of Buffer PB, centrifuged for 45 seconds at 13.000 rpm, and the flow through was discarded. 750 µL of Buffer PE was added to the spin column and the spin column was centrifuged for 45 seconds at 13.000 rpm to wash the column, remaining flow through was discarded. The solution was centrifuged for 1 min at 13.000 rpm to remove any remaining wash buffer. To elute the plasmid the spin column was placed in a 1.5 mL eppendorf tube and 50 µL Buffer EB was added in the centre of the spin column and the spin column was left to stand for 1 minute before it was centrifuged for 1 minute at 13.000 rpm.

2.3.4 In vitro transcription

All plasmid DNA were linearized at their respective restriction sites (Table 2.3).

Table 2.3: Plasmid DNA linearization

	Restriction Site	Buffer	Temp
pCS2 GFP	NotI	Cutsmart	37°C
pCS2 mCherry	NotI	Cutsmart	37°C
pTransposase	XbaI	Cutsmart	37°C
pUCIDT	BamHI	Cutsmart	37°C

Approximately 5 µg of isolated plasmid DNA was linearized. Plasmid DNA was mixed with 5 µL 10x Bovine Serum Albumin (BSA), 5 µL 10x Cutsmart enzyme buffer and 1 µL restriction enzyme corresponding to the restriction site for the plasmid DNA. Rnase-free H_2O was added to make the final volume for the reaction 50 µL. The reaction mix was incubated for 3 hours at 37°C. The enzyme reaction was purified using the MinElute Reaction Cleanup kit (Qiagen, USA) as described by the manufacturer.

Linearized plasmid DNA from pCS2 GFP, pCS2 mCherry, and pUCUDT was transcribed in vitro using ThermoFisher™ Invitrogen™ mMESSAGE mMACHINE® SP6 Transcription Kit. Linearized plasmid DNA from pTransposase was transcribed in vitro using ThermoFisher™ Invitrogen™ MEGAscript™ T3 Transcription Kit. 1 µg of the linearized plasmid DNA was transcribed as described by the manufacturer. Briefly, linearized plasmid DNA was mixed with 10 µL 2X NTP/CAP, 2 µL 10x reaction buffer, and 2 µL 10x enzyme mix. Rnase-free H_2O was added to make the final reaction 20 µL. The reaction was incubated for 4 hours at 37°C. After incubation 1 µL TURBO DNase was added and the mix was incubated for 15 minutes at 37°C. Transcribed mRNA was purified using Qiagen Rneasy mini kit (Qiagen, USA) as described by the manufacturer.

2.4 Gibson assembly

There are multiple methods for ligating DNA molecules together. Most of these methods rely on the use of restriction sites and "sticky ends". However, new ways of recombination circumvent this by blunt end cloning without depending on restriction enzyme sites [45]. The Gibson assembly provides a way to do this at one temperature in one reaction setup. The reaction does not require compatible restriction enzyme ends, instead predefined complimentary overhang sequences are used to anneal the two strands together after exonuclease digestion. Exonuclease digests from the 5' end towards the 3' end on both DNA molecules.

This digestion allows for the now partially single-stranded 3' ends on both molecules with complementary overhangs to anneal. After the two strands have annealed, DNA polymerase fills in the gaps left by the exonuclease digestion by polymerizing from the 3' ends, and ligase repairs the remaining gaps (Figure 2.3). Inserts containing the mutations were 60 bp long and its flanking overhang sequences of 30 bp each added up to a final oligonucleotide of 120 nucleotides. A complete list of all the oligonucleotides used in this study can be seen in table 2.4.

TABLE 2.4: List of all oligonucleotides ordered for the Gibson assembly. Underlined nucleotides represent the sequence overhang, while red lower-case letters represent sequence mutations.

trip10a WT	5'– ATAAGCTAGAACTATAGTGAGTCGTATTACAAATAATATAATT TATTGAGTAAATAAGCGCTTGTATATTAAATAAACATGTAT GTAAGAGTAGATCCAGACATGATAAGATACATTGAT –3'
trip10a WT Reverse	5'– ATCAATGTATCTTATCATGTCTGGATCTACTCTTACATACATG TTTATTTAATATACAAGCGCTTATTTACTCAATAAATTATA TTATTTGTAATACGACTCACTATAGTTCTAGCTTAT –3'
trip10a Mutation	5'– ATAAGCTAGAACTATAGTGAGTCGTATTACAAgcAAgcTAgcT gcTTGAGgcAAgcAaaGgTTGgcTATgcAAgcAACATGgcTGgcAGA GTAGATCCAGACATGATAAGATACATTGAT –3'
trip10a Mutation Reverse	5'– ATCAATGTATCTTATCATGTCTGGATCTACTCTgcCAgcCATG TTgcTTgcATAgcCAAcCttTgcTTgcCTCAAgcAgcTAgcTTgcTT GTAATACGACTCACTATAGTTCTAGCTTAT –3'
mx2.2 WT	5'– ATAAGCTAGAACTATAGTGAGTCGTATTACATATGTGAAGATT GTTGCTAATATTATTTAAAGTGACAAATGAAATAAAGGT TGTATCCAGTAGATCCAGACATGATAAGATACATTGAT –3'
mx2.2 WT Reverse	5'– ATCAATGTATCTTATCATGTCTGGATCTACTGGATACAACCTT TATTTCATTTGTCACTTTAAATAATATTAGCAACAATCTT CACATATGTAATACGACTCACTATAGTTCTAGCTTAT –3'
mx2.2 Mutation A	5'– ATAAGCTAGAACTATAGTGAGTCGTATTACATATGTGAAGATT GTTGCTAATATTgcTgcAAGTGACAAATGAgcTgcAGGTTGTATCCA GTAGATCCAGACATGATAAGATACATTGAT –3'
mx2.2 Mutation A Reverse	5'– ATCAATGTATCTTATCATGTCTGGATCTACTGGATACAACCTgc AgcTCATTTGTCACTTgcAgcAATATTAGCAACAATCTTCACATAT GTAATACGACTCACTATAGTTCTAGCTTAT –3'
mx2.2 Mutation B	5'– ATAAGCTAGAACTATAGTGAGTCGTATTACAgcTGTGAAGgcTG TTGCgcAgcTTgcTgcAAGTGACAAgcGAgcTgcAGGTTGgcTCCA GTAGATCCAGACATGATAAGATACATTGAT –3'
mx2.2 Mutation B Reverse	5'– ATCAATGTATCTTATCATGTCTGGATCTACTGGAgcCAACCTgc AgcTCgcTTGTCACTTgcAgcAAgcTgcGCAACAgcCTTCACAgcT GTAATACGACTCACTATAGTTCTAGCTTAT –3'

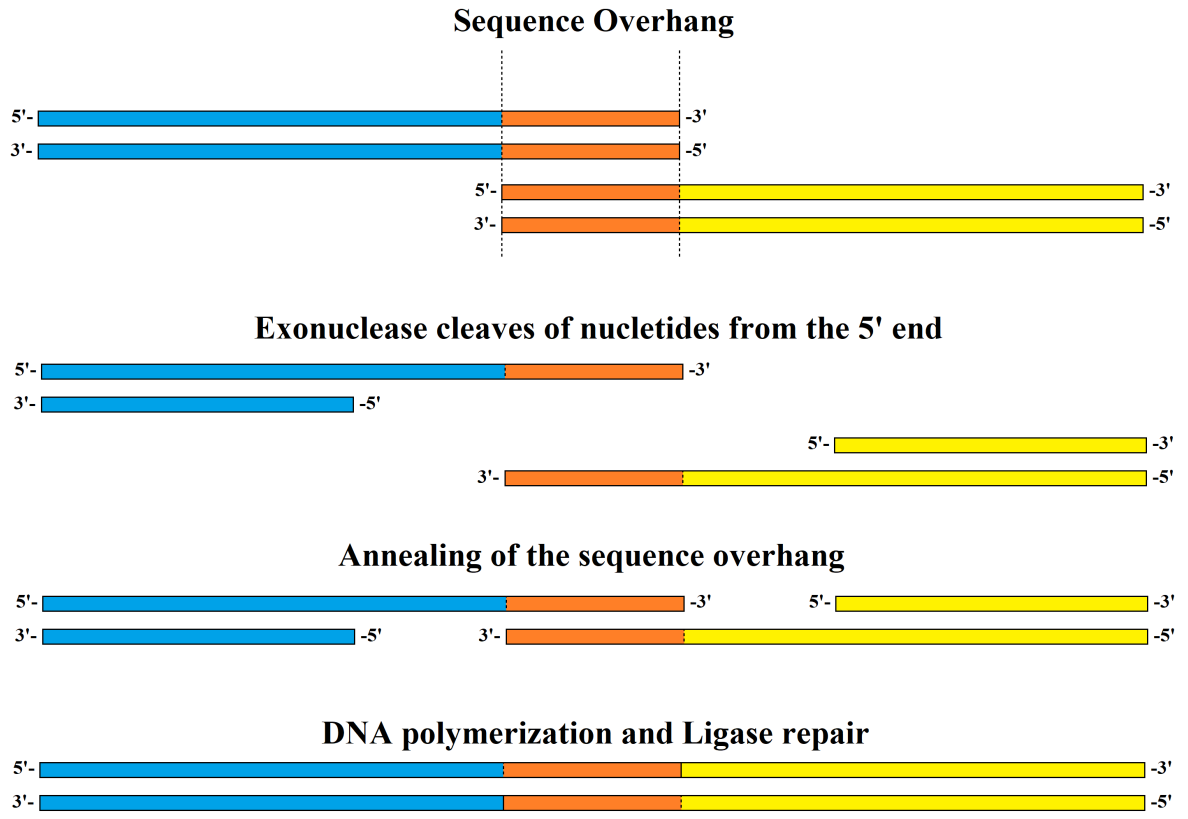

FIGURE 2.3: Two double-stranded DNA molecules (marked by blue and yellow) are ligated together by the Gibson assembly process. Exonuclease digests one of the DNA strands from the 5' end towards the 3' end on both DNA molecules. Complementary overhang sequences (orange) anneal the two DNA molecules together. DNA polymerase closes the gap and ligase seal the new ligated DNA molecule.

The single stranded oligonucleotides were annealed by preparing the reaction mix described in table 2.5.

TABLE 2.5: Annealing of oligonucleotides

	Oligo	Concentration
1 µL	F oligo	100 µM
1 µL	R oligo	100 µM
8 µL	MilliQ	
10 µL	Total volume	

The annealing reaction mix was incubated using the following program:

- 5 minutes at 95°C

- Ramping - 2°C per second to 85°C
- Ramping - 0.1°C per second to 25°C

The plasmid vector pCS2 GFP was linearized at the SnabI restriction site. Linearized vectors, 2.25 µL (100 ng), were added together with 1.5 µL of the insert fragment, 10 µL of Gibson assembly master mix and 6.25 µL dH_2O to a final reaction volume of 20 µL. The reaction was incubated at 50°C for 60 minutes. A control reaction containing 10 µL of NEBuilder(New England Biolabs, USA) positive control reagents and 10 µL of NEBuilder(New England Biolabs, USA) master mix was used as a positive control. Recombinant plasmids were transformed into TOPO10 competent cells as described in section 2.3.2, and plasmid DNA was isolated as described in section 2.3.3.

2.4.1 Sanger sequencing

To verify that the insert had successfully been incorporated into the DNA, the plasmid DNA was sequenced using Sanger sequencing. The sequencing was performed at the sequencing lab at the University of Bergen. Plasmid DNA was prepared for sequencing by mixing 1 µL of bigdye version 3.1, 1 µL 5x of seqbuffer, 1 µL M13 primer (3.2 pmol), 0.5 µL of DNA template (≈400 ng), and 6.5 µL of dH_2O. The reaction was thermocycled using the program described in table 2.6. After thermocycling 10 µL of dH_2O was added to the solution for a total solution of 20 µL.

TABLE 2.6: Program used on the thermocycler for Sanger sequencing.

	Cycle Step	**Temp** (°C)	**Time**	
1	Initial denaturation	96	5 min	
	Denaturation	96	30 s	} × 25 cycles
2	Annealing	50	30 s	} × 25 cycles
	Extension	60	45 s	} × 25 cycles
3	Hold	4	∞	

2.5 Agarose gel electrophoresis

Agarose was mixed with Tris-acetate-EDTA (40mM Tris, 20mM Acetate, and 1mM Ethylenediaminetetraacetic acid (EDTA)) (TAE buffer) to make a 1 % agarose gel. Agarose gel was run at 100 V submerged in TAE buffer. GelRed was used to visualise the bands in the gel. Agarose gel electrophoresis was used to verify linearization of plasmids and to verify mRNA transcripts.

2.6 Zebrafish maintenance and handling

Zebrafish were kept and maintained in the zebrafish facilities at the University of Bergen, Department of Biological Sciences. The facility houses a variety of zebrafish WT strains (AB, TAB, and SWT). Spotty wild type (SWT) and a mutant strain called *casper* were used for injections in the work on this thesis. Casper zebrafish exhibit a transparent phenotype [46] and thus makes it ideal for fluorescence imaging.

In the evening on the day before injection, after the zebrafish had been fed, male and females were separated in breeding boxes. The breeding box consisted of a main container with a secondary box stacked inside. The secondary box was fitted with a netlike metal wiring just big enough for eggs to fall through, but too small for the fish to enter. Males and females were separated overnight and joined together in the secondary box at 8 am after light came on. Within 10-30 minutes eggs would be produced and start falling through the metal wiring and accumulate at the bottom of the main container. Eggs were collected and rinsed with E3-medium (Table 2.7) before they were injected. 4-6 breeding boxes were prepared prior to each injection to ensure that enough eggs would be fertilized for injection.

TABLE 2.7: E3 embryo buffer reagents.

Reagents	Concentration
NaCl	5 mM
KCl mCherry	0.17 mM
$MgSO_4$	0.33 mM
$CaCl_2$	0.33 mM
Methylene blue	5-10% of volume

2.7 Zebrafish injection

A Picospritzer III (Parker Hannfin Corp, USA) nitrogen pressure system in combination with a micromanipulator (InjectMan NI 2, Eppendorf, Germany) was used to ensure reliable and precise injection of mRNA into zebrafish embryos. A Nikon SMZ-645 stereomicroscope (Nikon, Japan) provided magnification while the micromanipulator was used to control the needle. A Borosilicate glass cylinder(10 cm long with an outer diameter of 1.0 mm) with filament (Sutter Instrument, USA) was heat-pulled by an automatic needle-puller (Narishige, Japan) to form the needle for injections. 2.5-5 µL of the injection mix was inserted into the needle and the tip was carefully cracked open using a pair of forceps. Zebrafish embryos were injected with an injection mix containing 125 ng/µL pCS2 GFP mRNA and 75 ng/µL pCS2 mCherry mRNA. The volume of injected mRNA was calibrated using a 1 mm ruler imprinted on a glass disc embedded in a black anodized aluminium slide (Electron Microscopy Sciences, USA)(Figure 2.4a). Test injections were performed in mineral oil (Sigma-Aldrich, USA) and the diameter of the injected droplet that formed in the oil was measured on the ruler. This allowed for adjusting the pressure coming from the pressure system, thus increasing or decreasing the diameter of the droplet formed in the mineral oil. Injections in this study had a diameter of 0.2 mm (200 µm) which corresponds to 1 nL injection mix. Fertilized eggs were prepared for injection in an agarose mould (Figure 2.4c). Between 50-100 eggs were manually placed down side by side in the mould to achieve optimal injection efficiency. Embryos were injected before they reached the second cell stage, < 0.75 hpf. The injection mix was injected into the yolk of the zebrafish egg and care was taken to inject as close to the developing cell as

possible (Figure 2.4b). After injection the embryos were collected in Petri dishes, about 50 embryos per Petri dish, and incubated at 28°C.

2.8 Fluorescent microscopy and image quantification

Expression of GFP and RFP was observed in all injected zebrafish embryos, however at varying intensities. Injected embryos were initially scanned for RFP fluorescence using a Zeiss SteREO Lumar V12 stereomicroscope, and selected based on clearly visible and comparable levels of RFP fluorescence. During RFP selection, care was taken to ensure that levels of RFP fluorescence were as consistent as possible between selected individuals. 18 embryos for each construct were selected for further imaging. For imaging, embryos were dechorionated and placed individually in a 6-welled plate so that the individual embryos could be imaged at different time points. Embryos were imaged at either at 6-12-24 hpf, 12-24-48 hpf, or 24-48-72-96-120 hpf. Images was taken at two different fluorescent channels, GFP and mCherry (Figure 2.5), at 5x magnification. After initial scanning for RFP, embryos were imaged using a Leica DM6000 B Microscope equipped with a DFC350FX R2 camera for both RFP and GFP. Settings for imaging were explored early in the process and standardized at 1 second exposure. mCherry absorbs light at 587 nm and emits light at 610 nm. GFP absorbs light at 489 nm and emits light at 509 nm. Embryos were sedated prior to imaging due to twitching, at 24 hpf, and general movement at 48 hpf and later. Embryos were placed in a Petri dish with fish water and Tricaine (0.016 %) was used as a sedative. For embryos at 24 hpf the sedative would take effect within seconds of exposure. However for 48 hpf and older, the tricaine needed longer to make an effect, sometimes up to 2-3 minutes. After imaging the embryos were placed back into its well in fresh E3 medium without sedative.

All images were analysed using the ImageJ software. Each image was opened in ImageJ as a .tif file with a resolution of 1392x1040 pixels. The image was analysed as a two dimensional image where each vertical line of pixels in the image was given an average

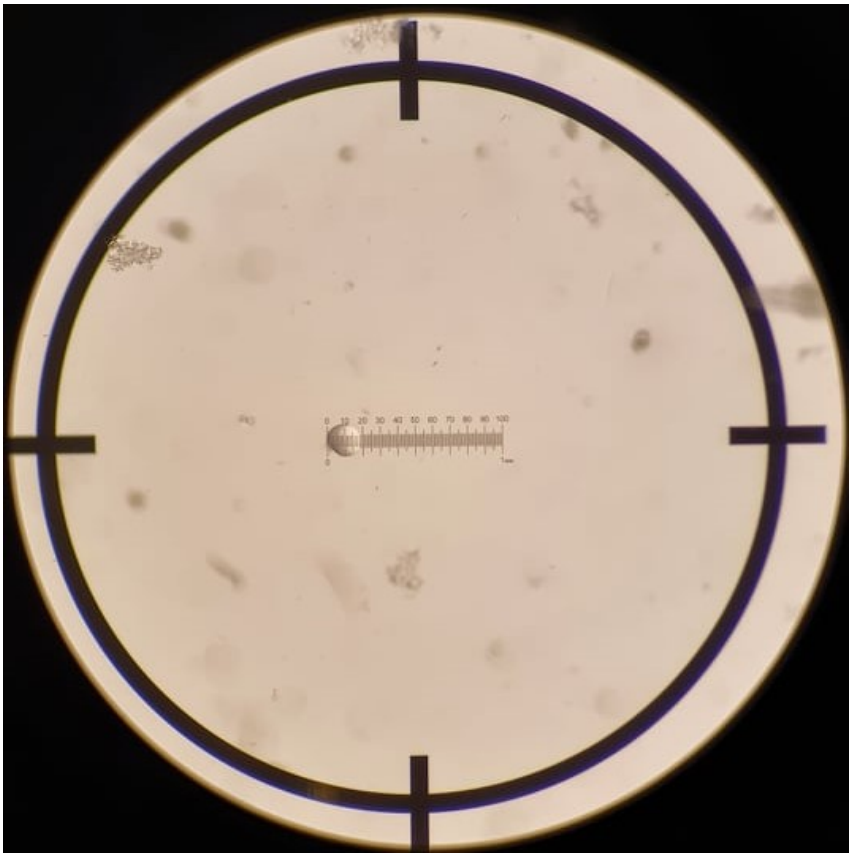

(a) 1 mm ruler imprinted on a glass disc embedded in a black anodized aluminium slide (Electron Microscopy Sciences, USA)

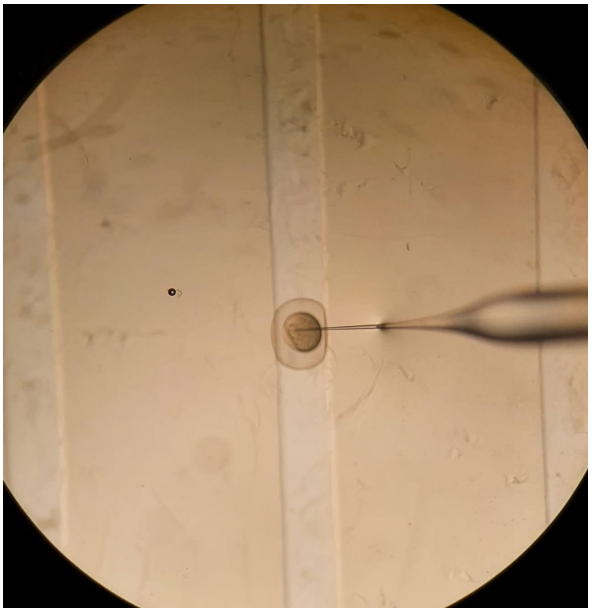

(b) Injection of zebrafish embryo at the single-cell stage.

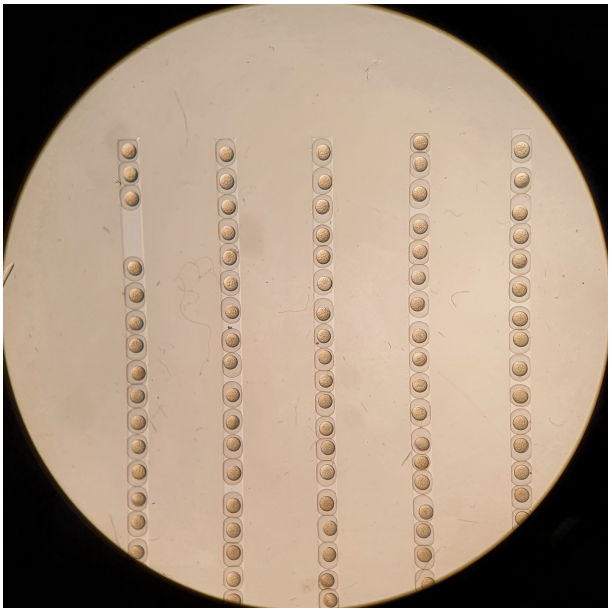

(c) Overview of zebrafish embryos lined up in an agar mould for injection.

FIGURE 2.4: Overview over different parts used in the injection of zebrafish.

(a) Zebrafish under white light.

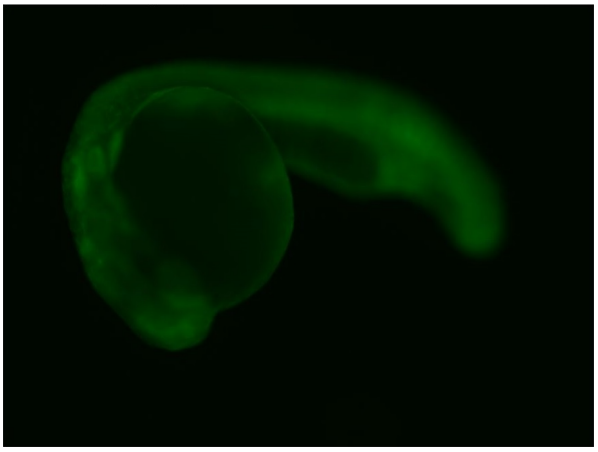

(b) GFP fluorescence.

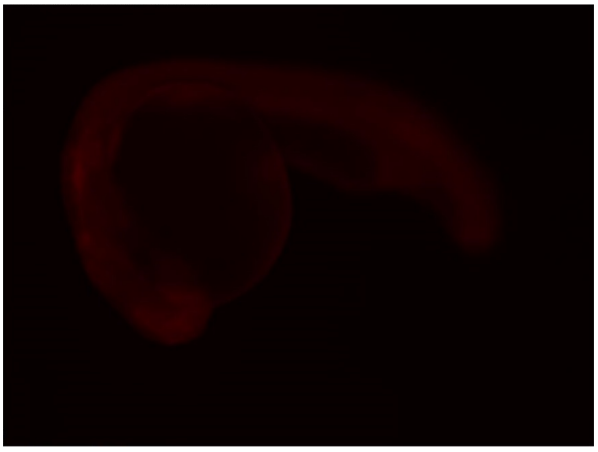

(c) RFP fluorescence.

FIGURE 2.5: Different use of filters for fluorescence.

value of all the colours in the line, in total 1392 vertical lines (Figure 2.6). The values for all the resulting lines were plotted, and a unique fluorescence profile for each image was created (Figure 2.6c). Images initially displayed some background fluorescence (Figure 2.6b), and this was subtracted from the image. The area under each graph for each image was calculated and the negative control was subtracted from this value.

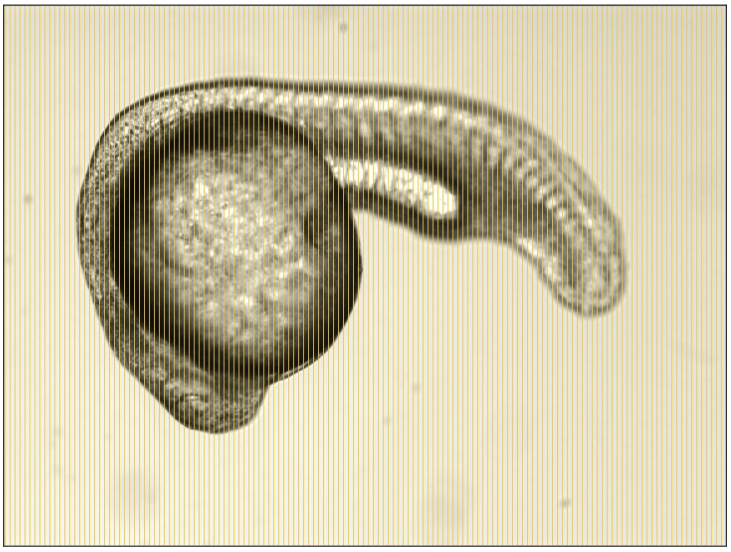

(a) Image divided into vertical lines along the x-axis. A total of 1392 lines recieved its own value.

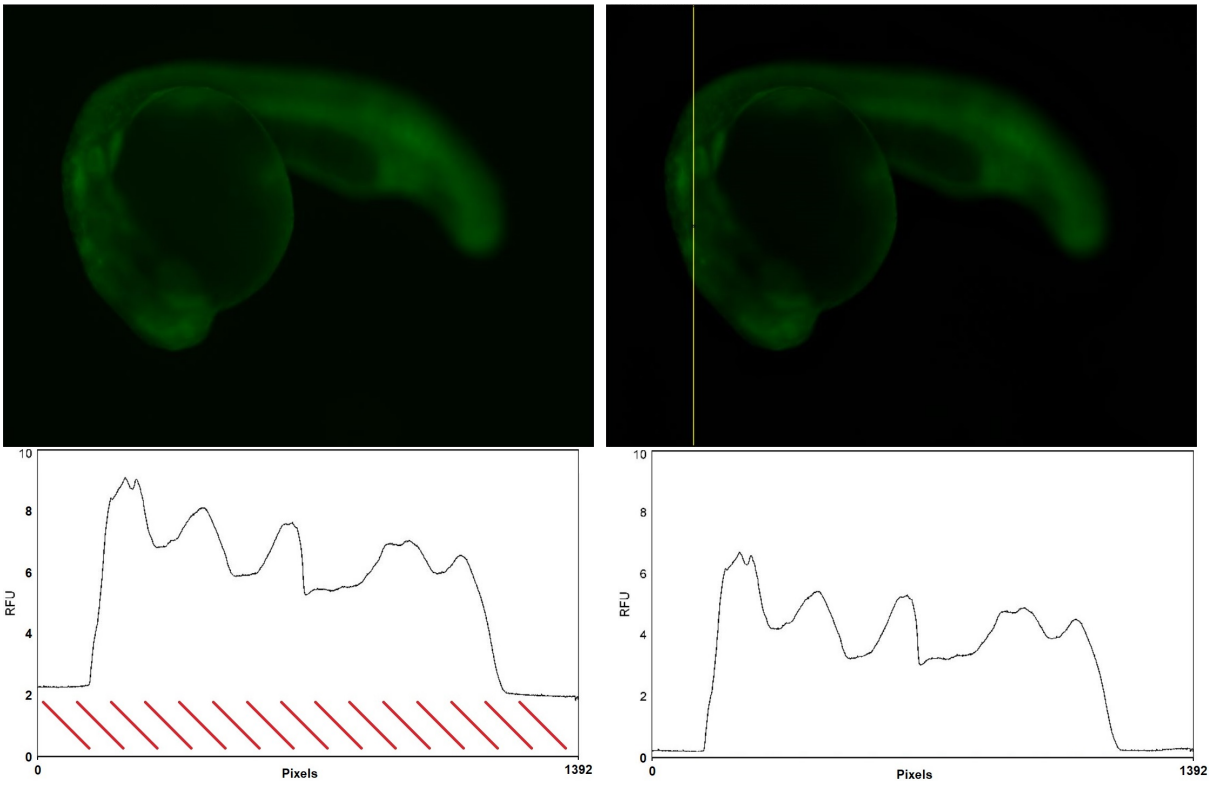

(b) Plot without subtracted background fluorescence (Slanted red lines).

(c) Plot showing background fluorescence after subtraction.

FIGURE 2.6: Image Analysis and Quantification by ImageJ.

2.9 Statistical analysis

Significant differences between groups were identified using an unpaired single tailed Students t-test. Significance levels were kept at $p < 0.05$ for all tests ($* \; p < 0.05$; $** \; p < 0.01$).

Results

3.1 GFP and RFP expression vectors

GFP was observed from all three of the plasmid vectors tested (Figure 3.1). Injected mRNA from pCS2 GFP and pUCIDT showed uniform levels of fluorescence throughout the zebrafish body, while the pTransposase/pDestTol2 system showed GFP fluorescence mainly in the zebrafish yolk and random restricted regions of fluorescence in the body. GFP fluorescence from the pTransposase/pDestTol2 system was in addition to this more intense. Images from the pTransposase/pDestTol2 system (Figure 3.1b) had to be taken using an exposure time of only 50 ms to avoid overexposure, while images of pCS2 GFP and pUCIDT fluorescence could be taken at 1 s exposure time without overexposure (Figure 3.1a and 3.1c).

Initial assessment of injected mRNA concentration was done by injecting embryos with 25 ng/µL and 250 ng/µL mRNA (Figure 3.2). This showed faint levels of GFP fluorescence at 25 ng/µL in both the transcribed mRNA from the pCS2 GFP and pUCIDT plasmid vectors. GFP fluorescence levels increase with increased mRNA concentration, and at 250 ng/µL GFP fluorescence is clearly visible.

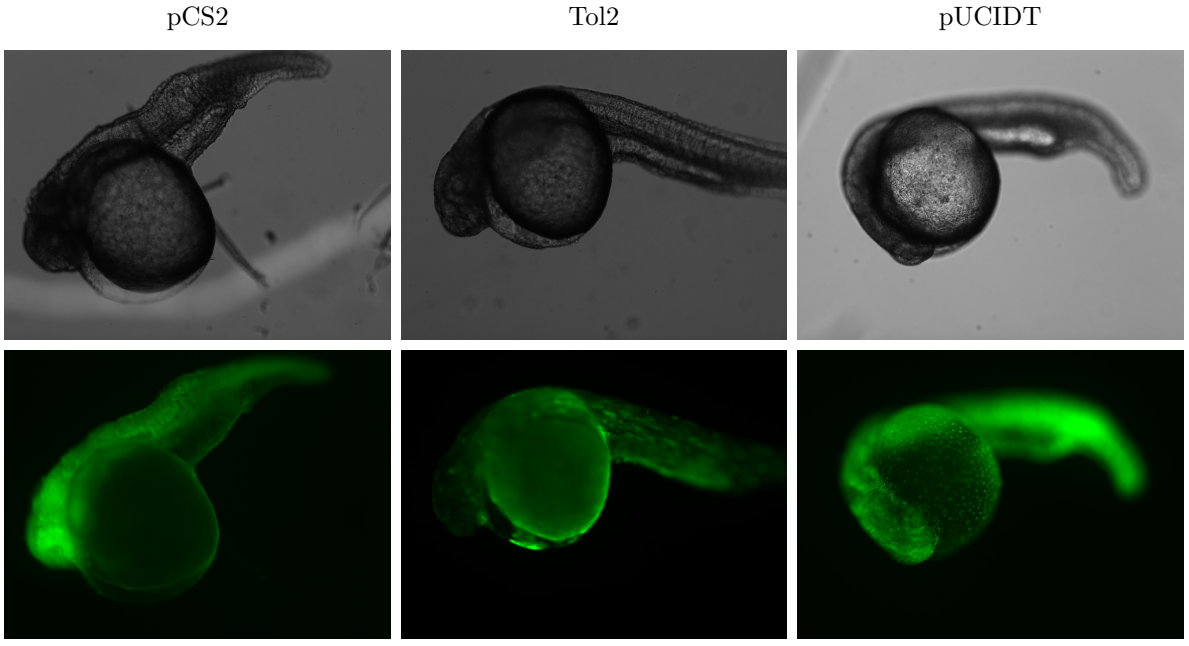

FIGURE 3.1: Initial testing of the three vectors; pCS2 mt-GFP (BamHI minus), pDest-Tol2pA2_ubiEGFP and pUCIDT for gfp expression. Zebrafish eggs were injected with 250 ng/µL of each vector and the images were taken 24 hpf. Images of pCS2 and pUCIDT were taken with an exposure time of 1 s, while the image of Tol2 was taken at 50 ms.

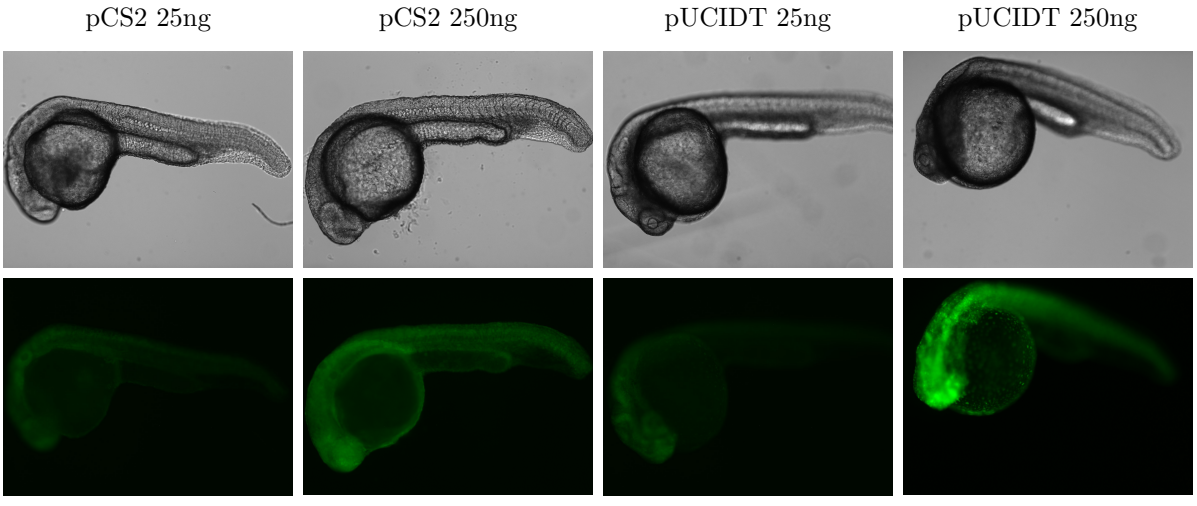

FIGURE 3.2: In order to determine the concentration of the injection mix, the pCS2 and pUCIDT vectors were both tested at 25 ng/µL and 250 ng/µL. Images were taken at the same exposure settings at 24 hpf.

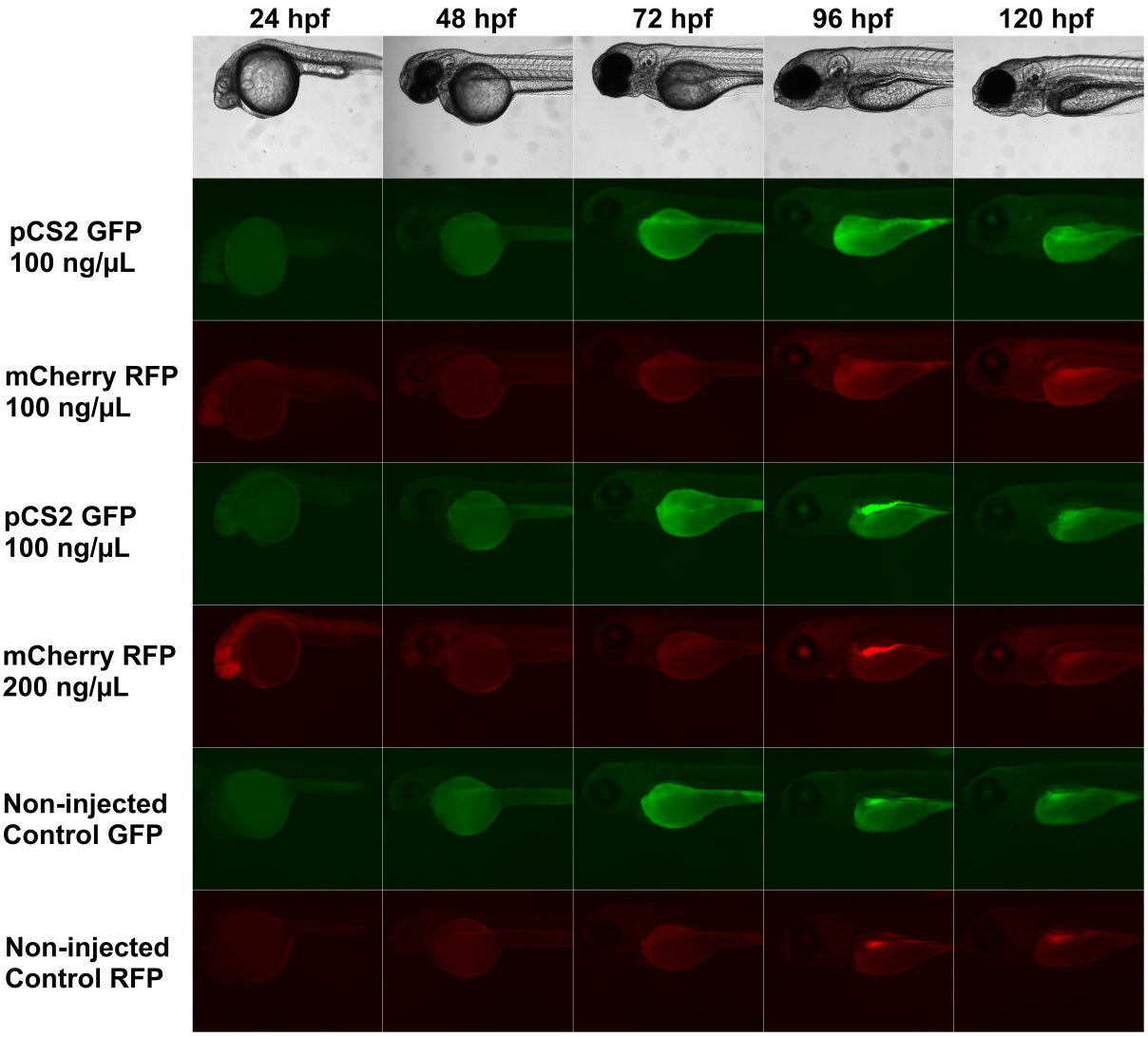

FIGURE 3.3: Comparison between RFP fluorescence levels from zebrafish embryos injected with 100 ng/µL pCS2 mCherry and 100 ng/µL pCS2 GFP and RFP fluorescence levels from embryos injected with 200 ng/µL pCS2 mCherry and 100 ng/µL pCS2 GFP.

Concentration of injected pCS2 RFP mRNA was assessed at 100 ng/µL and 200 ng/µL to get a sense of the RFP fluorescene and how this compared to the fluorescence intensity of GFP. When concentration of pCS2 GFP mRNA was kept at 100 ng/µL, pCS2 RFP mRNA fluorescence levels were comparable to pCS2 GFP mRNA fluorescence levels (Figure 3.3), and thus the concentration of injected pCS2 GFP mRNA and pCS2 mCherry mRNA were within the same range. There was an increase in RFP fluorescence as the pCS2 mCherry mRNA concentration was increased from 100 ng/µL to 200 ng/µL. Difference in fluorescence of RFP between the two concentrations was most apparent at

24 hpf. RFP fluorescence levels were almost identical for both concentrations, post 24 hpf. Autofluorescence was observed at 48 hpf and increased as the zebrafish got older, particularly in the yolk and later in the gut of the zebrafish.

3.2 *trip10a* and *mx2.2* 3'UTR expression constructs

The mutated *trip10a* sequence contained 7 mutations in the two AREs, ATTTA and AAATAAA. In addition to mutations in these two AREs, 14 mutations were done in selected TA sequences throughout the insert, and two mutations in a potential ARE AAATAA. The 3'UTR in the *mx2.2* gene were searched for the regulatory elements proposed by Vejnar et al. [16]. Based on this and observations done by mutating the *trip10a* sequence, we located a stretch of two putative AREs, ATTTA and AAATAAA in the *mx2.2*.

FIGURE 3.4: List of all the five inserts ligated into the 3'UTR region of a pCS2 GFP vector. In the WT inserts regions of interest are marked with green, ATTTA and AAATAAA are AREs, AAATAA and ATTTATT are potential AREs, while AAGCGCTT marks a potential microRNA site. Mutations are marked with lower-case red letters.

The *mx2.2* insert were mutated in two different versions, mutation A and mutation B. The *mx2.2* mutation A sequence contained 8 mutations in the two AREs, ATTTA and

AAATAAA. In addition, in mutation B, 12 mutations were done in selected TA sequences throughout the insert.

Oligos from 3'UTR in *trip10a* and *mx2.2*, both wt and mutated version, were ligated into the 3'UTR region of the pCS2 GFP vector. To verify correct insertion of the regulatory 3'UTR elements, we sequenced purified plasmid clones from each ligation experiment. Results from the Sanger sequencing showed that inserts had been successfully inserted into the pCS2 GFP vector (Figure 3.4).

3.3 Standardizing a control baseline

Measurements of background fluorescence in non-injected embryos across experiments were collectedby quantification of fluorescence intensity by using the ImageJ software and a mean fluorescence baseline was established (Tables 3.1 and 3.2).

TABLE 3.1: Measurement of GFP fluorescence of non-injected controls. Controls were sampled from multiple experiments and a mean baseline of GFP fluorescence for the non-injected controls at different time points were established.

	6 hpf	12 hpf	24 hpf	48 hpf	72 hpf	96 hpf	120 hpf
Negative control 1	5.93	10.12	10.18	-	-	-	-
Negative control 2	5.70	8.59	9.17	-	-	-	-
Negative control 3	6.14	9.40	9.49	-	-	-	-
Negative control 4	-	-	7.99	14.15	19.96	20.73	18.43
Negative control 5	-	-	9.39	13.94	19.67	23.19	25.10
Negative control 6	-	7.64	7.77	12.05	-	-	-
Negative control 7	-	8.39	8.52	16.89	-	-	-
Mean	5.92	8.83	8.93	14.26	19.82	21.96	21.77
SD	0.18	0.85	0.81	1.73	0.14	1.23	3.34

Measured background fluorescence showed little variation between individuals. An increase in background fluorescence levels is observed over time from 6 hpf - 120 hpf due to the onset of autofluorescence, as expected.

TABLE 3.2: Measurement of RFP fluorescence of non-injected controls. Controls were sampled from multiple experiments and a mean baseline of RFP fluorescence for the non-injected controls at different time points were established.

	6 hpf	12 hpf	24 hpf	48 hpf	72 hpf	96 hpf	120 hpf
Negative control 1	5.88	7.68	6.68	-	-	-	-
Negative control 2	5.53	6.36	5.73	-	-	-	-
Negative control 3	5.44	7.19	6.81	-	-	-	-
Negative control 4	-	-	5.68	7.97	10.63	12.31	13.02
Negative control 5	-	-	6.20	7.70	10.34	14.38	22.82
Negative control 6	-	5.44	5.29	7.08	-	-	-
Negative control 7	-	6.43	5.77	9.05	-	-	-
Mean	5.62	6.62	6.02	7.95	10.48	13.35	17.92
SD	0.19	0.77	0.52	0.71	0.15	1.03	4.90

3.4 mRNA 3'UTR regulative elements in *trip10a*

Embryos injected with pCS2 GFP mRNA containing the mutated *trip10a* 3'UTR insert showed visually stronger levels of fluorescence over embryos injected with pCS2 GFP mRNA containing the WT *trip10a* 3'UTR insert after normalization against pCS2 mCherry fluorescence (Figure 3.5 - 3.7). Images taken at 24, 48, 72, 96, and, 120 hpf (Figure 3.5) showed that fluorescence intensity at 24 hpf is stronger for the mutation, however fluorescence decreases and autofluorescence becomes apparent somewhere between 24 and 48 hpf. Gradual decline of fluorescence in the zebrafish body was observed from 24 hpf all the way to 120 hpf, while autofluorescence in the yolk increases. The decline of fluorescence as early as 48 hpf suggests that the peak of GFP expression might be at 24 hpf or earlier. Subsequent images taken at 6, 12 and, 24 hpf showed that strong fluorescence of GFP occurs earlier than 24 hpf, even as early as 6 hpf (Figure 3.6). It is also apparent that background autofluorescence is minimal at this stage of zebrafish development. Images of GFP fluorescence at 6 and 12 hpf show higher fluorescence intensity in zebrafish injected with mRNA containing the mutated *trip10a* 3'UTR insert compared with the WT *trip10a* 3'UTR insert. GFP and RFP fluorescence varied somewhat between individuals, however GFP fluorescence of the mutant was consistently higher than GFP fluorescence in the WT (Figure 3.7). This image shows fluorescence of GFP and RFP at

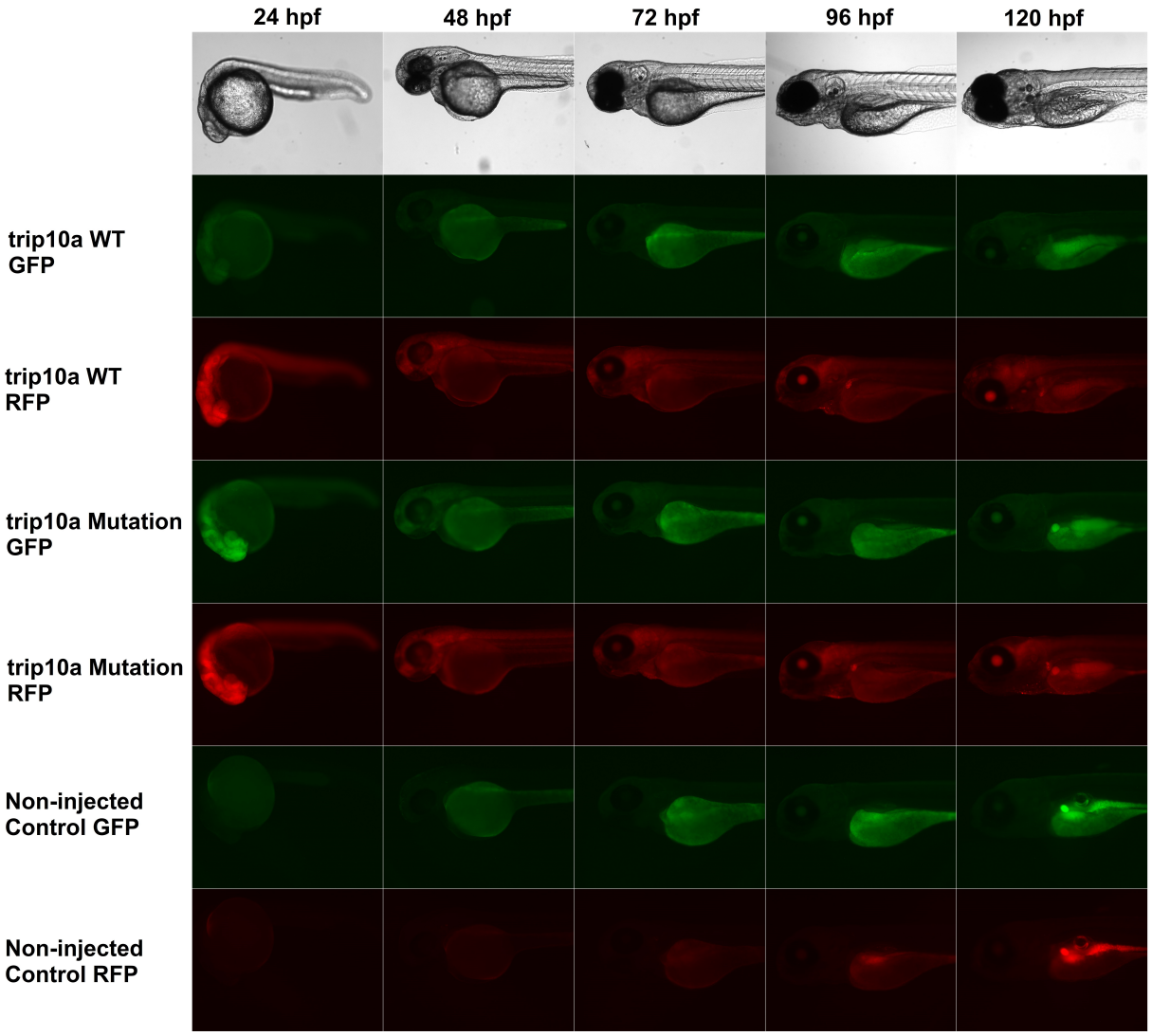

FIGURE 3.5: Images taken at 24, 48, 72, 96 and 120 hpf of GFP and RFP fluorescence levels of zebrafish injected with mRNA with *trip10a* WT and mutated inserts in their 3'UTR.

24 hpf for five individuals with the mutated insert and 5 five individuals with the WT insert.

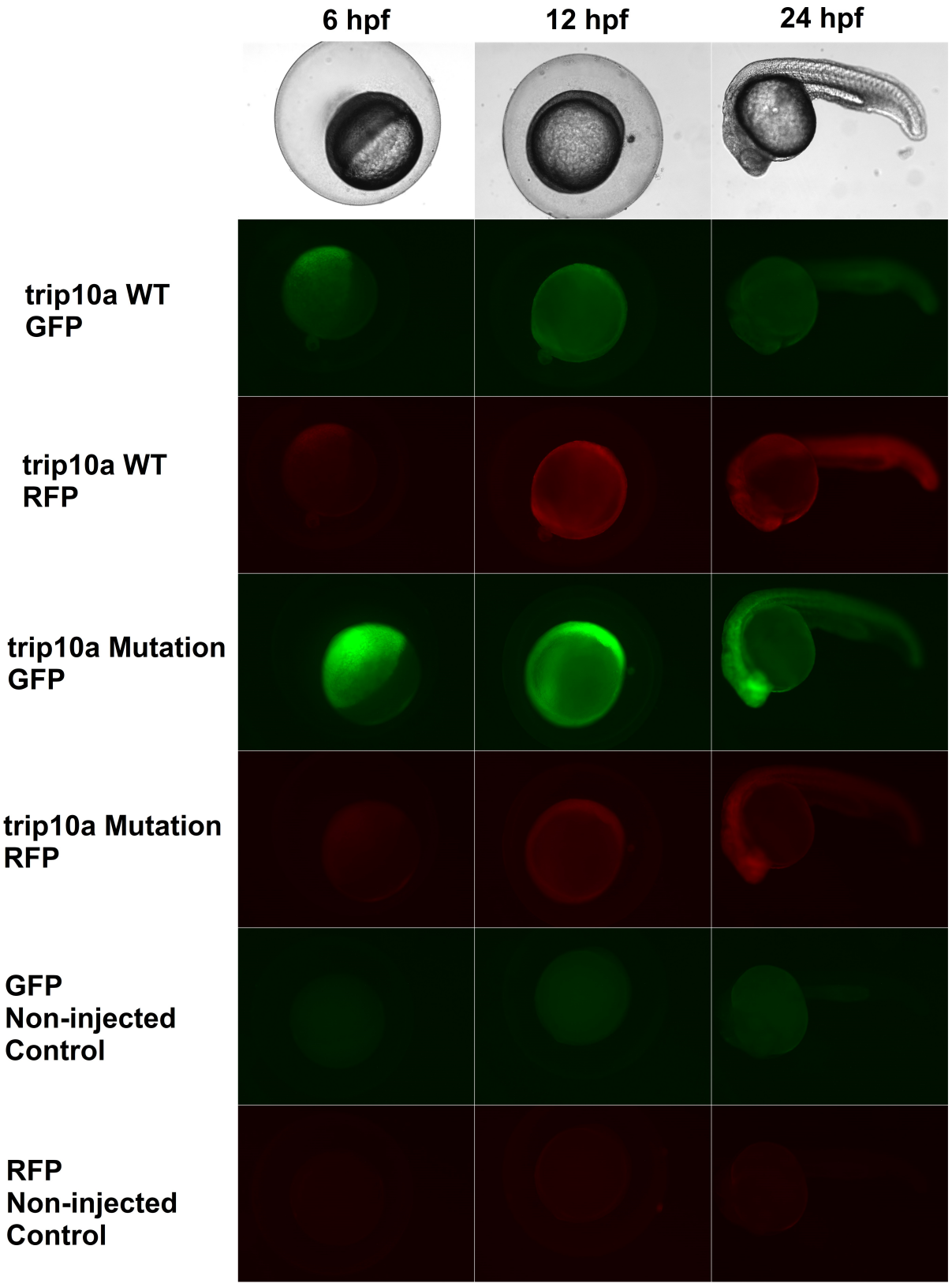

FIGURE 3.6: Images taken at 6, 12 and 24 hpf of GFP and RFP fluorescence levels of zebrafish injected with mRNA with *trip10a* WT and mutated inserts in their 3'UTR.

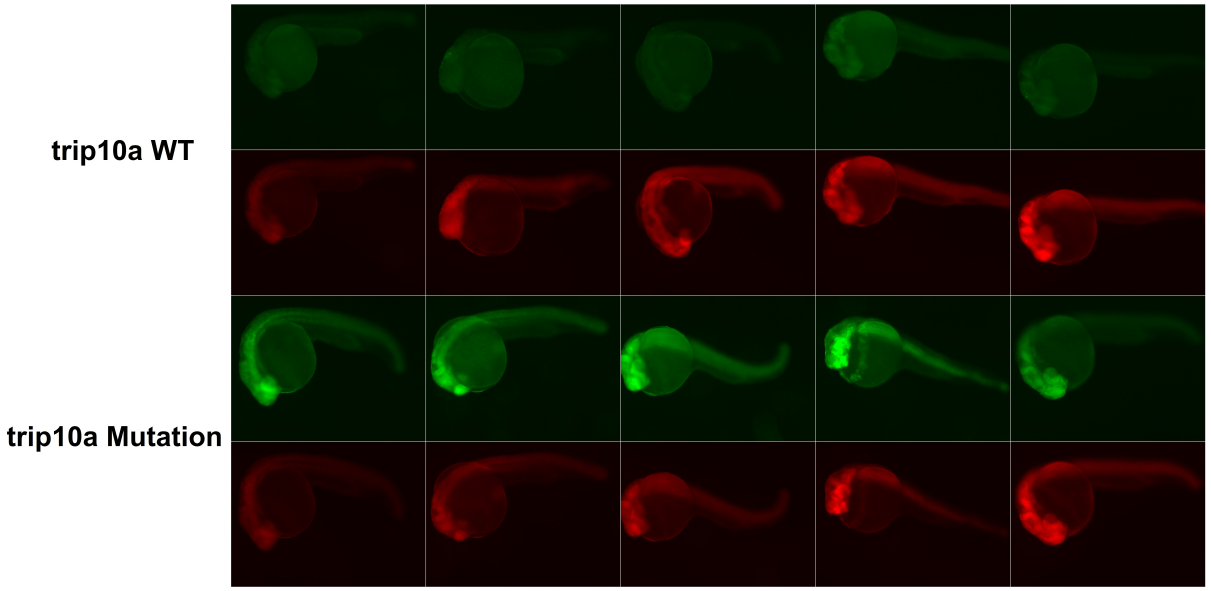

FIGURE 3.7: Images taken at 24 hpf of GFP and RFP fluorescence levels of zebrafish injected with mRNA with *trip10a* WT and mutated inserts in their 3'UTR.

18 individuals with the mutated insert and 18 individuals with the WT insert were planned for imaging at 24, 48, 72, 96, and 120 hpf, and subsequent analysis and quantification (Table 3.4). At 24 hpf two of the WT individuals had died, and four of the mutated individuals died. Further twelve WT individuals and three mutated individuals had died at 48 hpf. In total 16 images of the WT insert and 14 images of the mutated insert were analysed at 24 hpf. 4 images of the WT insert were analysed at all five time points, while 11 images of the mutated insert were analysed at all five time points. Quantification of fluorescent intensity by analysis of images using ImageJ showed a significantly higher fluorescence levels of pCS2 GFP mRNA containing the mutated *trip10a* 3'UTR insert over pCS2 GFP mRNA containing the WT *trip10a* 3'UTR insert at 24 hpf (Figure 3.8a). Fluorescent intensity showed decreased over time from 48 hpf (Figures 3.8b-3.8e). However, fluorescent intensity appears to be consistent from 6 hpf to 24 hpf. Fluorescence values were significant at 24 hpf ($p < 1.19291E-09$), at 48 hpf ($p < 2.91923E-06$), at 72 hpf ($p < 0.008$) and at 120 hpf ($p < 0.002$). Fluorescence values were not significantly higher at 96 hpf ($p < 0.16$).

TABLE 3.3: Measured fluorescence levels from the second *trip10a* experiment at 6, 12 and 24 hpf. Measured fluorescence has been refined and normalized against RFP fluorescence levels.

	6 hpf	12 hpf	24 hpf
trip10a-WT 1	5.06	4.48	6.97
trip10a-WT 2	7.60	8.20	8.66
trip10a-WT 3	7.29	7.45	8.34
trip10a-WT 4	5.75	5.72	x
trip10a-WT 5	7.96	6.04	7.74
trip10a-WT 6	6.81	5.39	6.63
trip10a-Mut 1	65.91	53.44	53.27
trip10a-Mut 2	54.01	53.24	53.95
trip10a-Mut 3	47.19	43.63	48.45
trip10a-Mut 4	30.44	29.05	30.49
trip10a-Mut 5	35.26	42.95	47.11
trip10a-Mut 6	26.21	32.64	33.36

6 individuals with the mutated insert and 6 individuals with the WT insert were planned for imaging at 6, 12, and, 24 hpf, and subsequent analysis and quantification (Table 3.3).

All individuals were alive throughout all the time points, except one individual in the WT group which had died at 24 hpf. Fluorescent intensity from images taken at 6 - 24 hpf also showed significantly higher levels of fluorescence in pCS2 GFP mRNA containing the mutated *trip10a* 3'UTR insert over pCS2 GFP mRNA containing the WT *trip10a* 3'UTR insert (Figure 3.9). Fluorescence values were significant at 6 hpf ($p < 0.001$), at 12 hpf ($p < 0.0001$) and at 24 hpf ($p < 0.0001$).

TABLE 3.4: Measured fluorescence levels from the first *trip10a* experiment at 24, 48, 72, 96 and 120 hpf. Measured fluorescence has been refined and normalized against RFP fluorescence levels.

	24 hpf	48 hpf	72 hpf	96 hpf	120 hpf
trip10a-WT 1	-36.63	x	x	x	x
trip10a-WT 2	5.84	4.30	3.83	4.11	1.02
trip10a-WT 3	5.55	x	x	x	x
trip10a-WT 4	3.31	x	x	x	x
trip10a-WT 5	4.69	x	x	x	x
trip10a-WT 6	4.21	x	x	x	x
trip10a-WT 7	7.59	x	x	x	x
trip10a-WT 8	4.70	1.87	0.66	-0.06	-0.39
trip10a-WT 9	7.04	x	x	x	x
trip10a-WT 10	5.58	x	x	x	x
trip10a-WT 11	4.16	2.70	1.18	0.04	-1.05
trip10a-WT 12	x	x	x	x	x
trip10a-WT 13	5.24	x	x	x	x
trip10a-WT 14	4.44	x	x	x	x
trip10a-WT 15	5.78	x	x	x	x
trip10a-WT 16	x	x	x	x	x
trip10a-WT 17	5.70	3.52	1.85	0.67	-1.22
trip10a-WT 18	5.27	x	x	x	x
trip10a-Mut 1	19.07	11.09	5.52	3.32	2.41
trip10a-Mut 2	21.05	x	x	x	x
trip10a-Mut 3	x	x	x	x	x
trip10a-Mut 4	13.71	7.77	4.72	3.91	2.18
trip10a-Mut 5	15.77	9.45	3.41	3.51	1.99
trip10a-Mut 6	13.83	7.84	3.49	1.92	2.93
trip10a-Mut 7	x	x	x	x	x
trip10a-Mut 8	21.21	11.93	6.51	0.04	-70.34
trip10a-Mut 9	18.44	10.07	6.54	3.39	4.66
trip10a-Mut 10	20.16	11.11	5.41	3.30	2.36
trip10a-Mut 11	12.79	6.29	1.91	1.71	1.60
trip10a-Mut 12	18.95	x	x	x	x
trip10a-Mut 13	12.58	7.10	2.94	0.95	0.19
trip10a-Mut 14	x	x	x	x	x
trip10a-Mut 15	14.55	x	x	x	x
trip10a-Mut 16	x	x	x	x	x
trip10a-Mut 17	22.41	11.81	4.58	0.48	0.12
trip10a-Mut 18	21.76	12.64	6.36	3.65	3.57

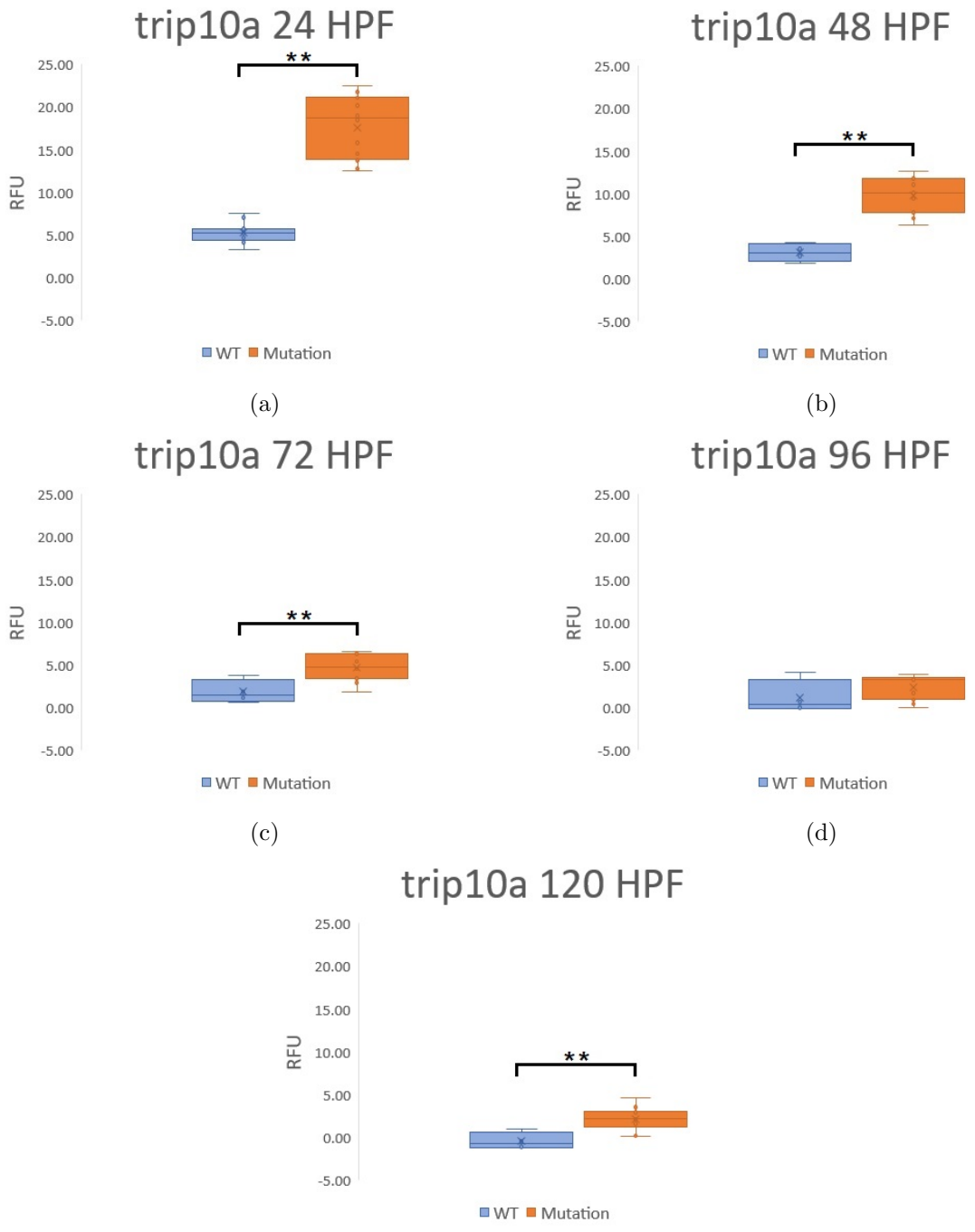

FIGURE 3.8: Boxplots showing the difference of fluorescence levels of mRNA injected with the *trip10a* WT insert and mutated insert. GFP fluorescence values has been normalized against RFP fluorescence values. a) Fluorescence levels at 24 hpf, b) fluorescence levels at 48 hpf, c) fluorescence levels at 72 hpf, d) fluorescence levels at 96 hpf and e) fluorescence levels at 120 hpf

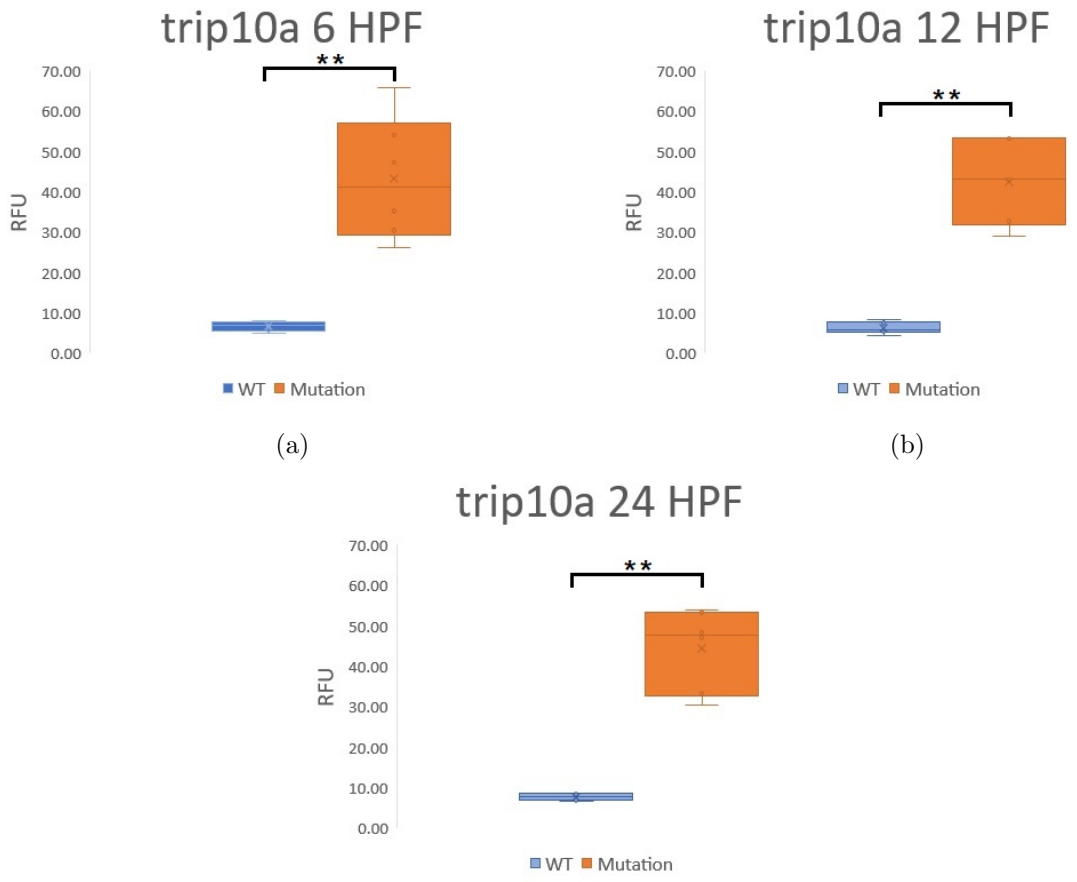

FIGURE 3.9: Boxplots showing the difference of fluorescence levels of mRNA injected with the *trip10a* WT insert and mutated insert. GFP fluorescence values has been normalized against RFP fluorescence values. a) Fluorescence levels at 6 hpf, b) fluorescence levels at 12 hpf and c) fluorescence levels at 24 hpf

3.5 mRNA 3'UTR regulative elements in *mx2.2*

Embryos injected with GFP mRNA containing the salmon gene *mx2.2* 3'UTR insert showed similar levels of fluorescence GFP in the two mutated 3'UTR inserts (mutation A and mutation B, Figure 3.10). No clear differences could be determined whether mutation A and mutation B showed higher GFP fluorescence than *mx2.2* WT 3'UTR insert (Figures 3.11 and 3.12). Embryos injected with GFP mRNA containing the salmon gene *mx2.2* WT 3'UTR insert showed higher fluorescence levels of GFP than imaged taken from the *trip10a* WT, and the fluorescence of GFP was closer to the levels of the mutated embryos.

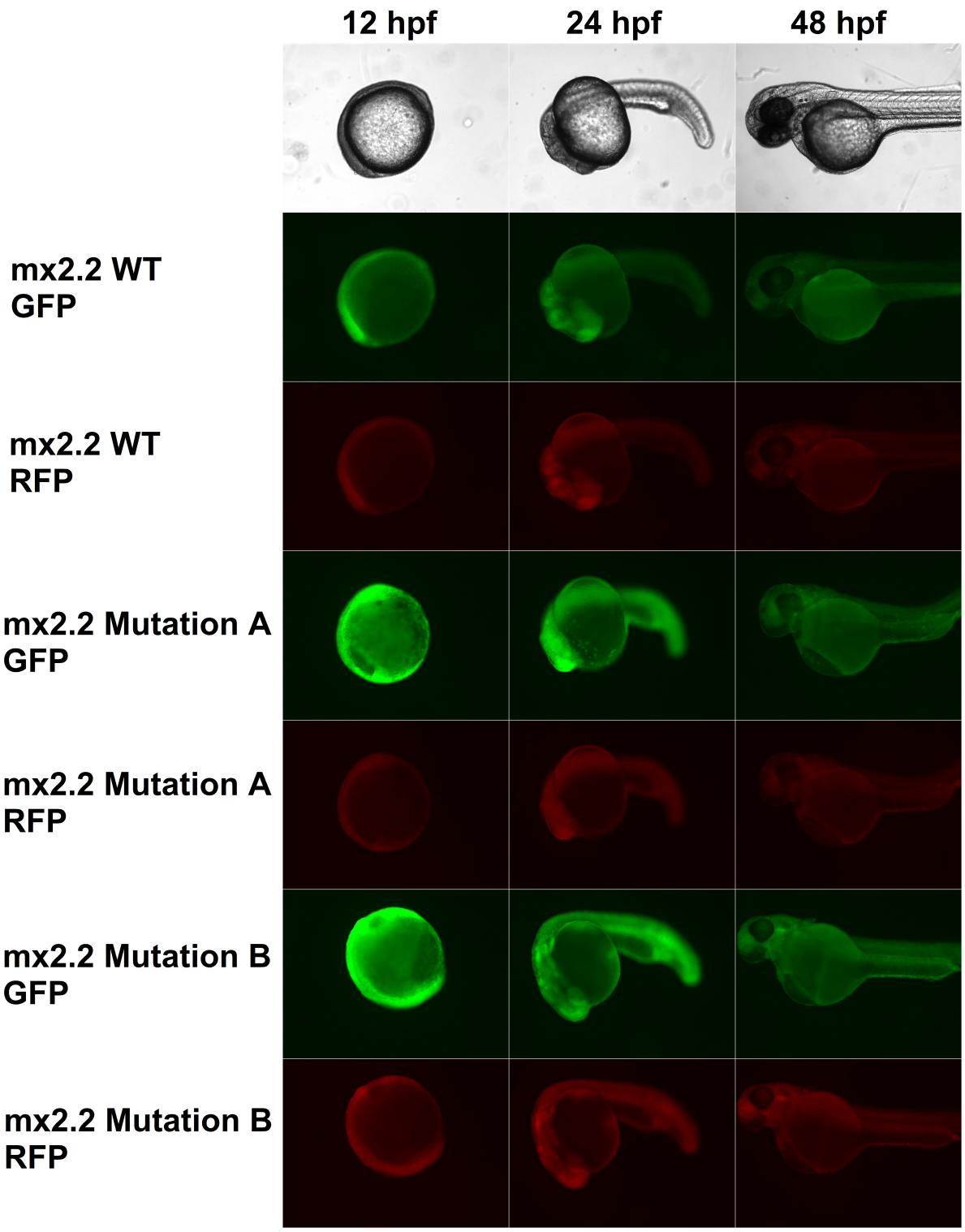

FIGURE 3.10: Images taken at 12, 24 and 48 hpf of GFP and RFP fluorescence levels of zebrafish injected with mRNA with *mx2.2* WT and mutation A and B inserts in their 3'UTR.

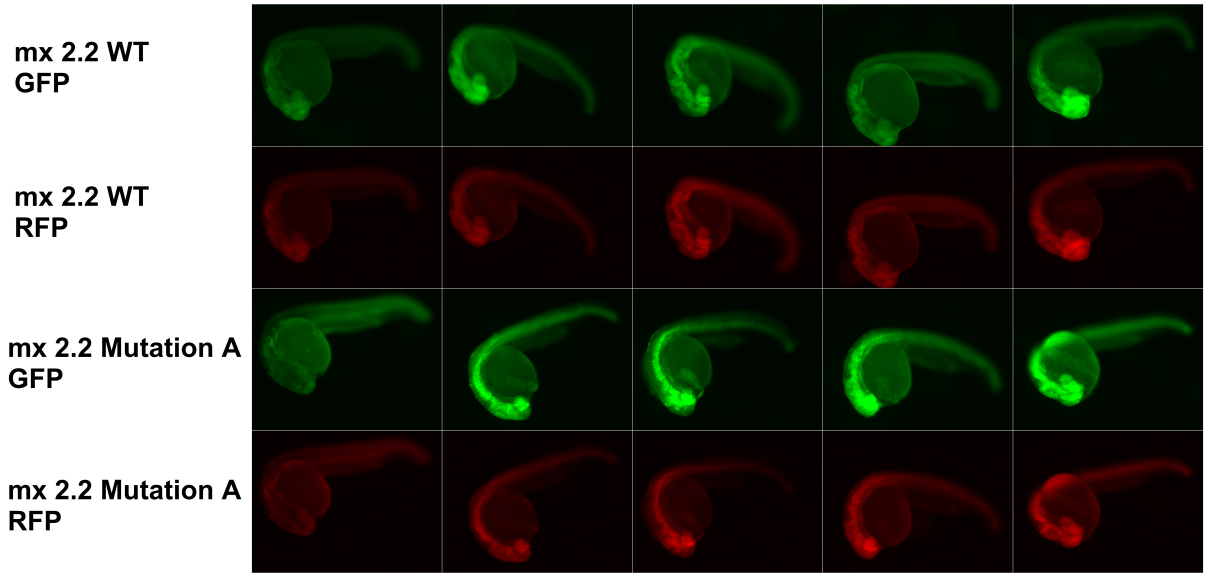

FIGURE 3.11: Images taken at 24 hpf of GFP and RFP fluorescence levels of zebrafish injected with mRNA with *mx2.2* WT and mutation A insert in their 3'UTR. Image shows 5 different individuals for the WT insert and 5 different individuals for the mutation A insert.

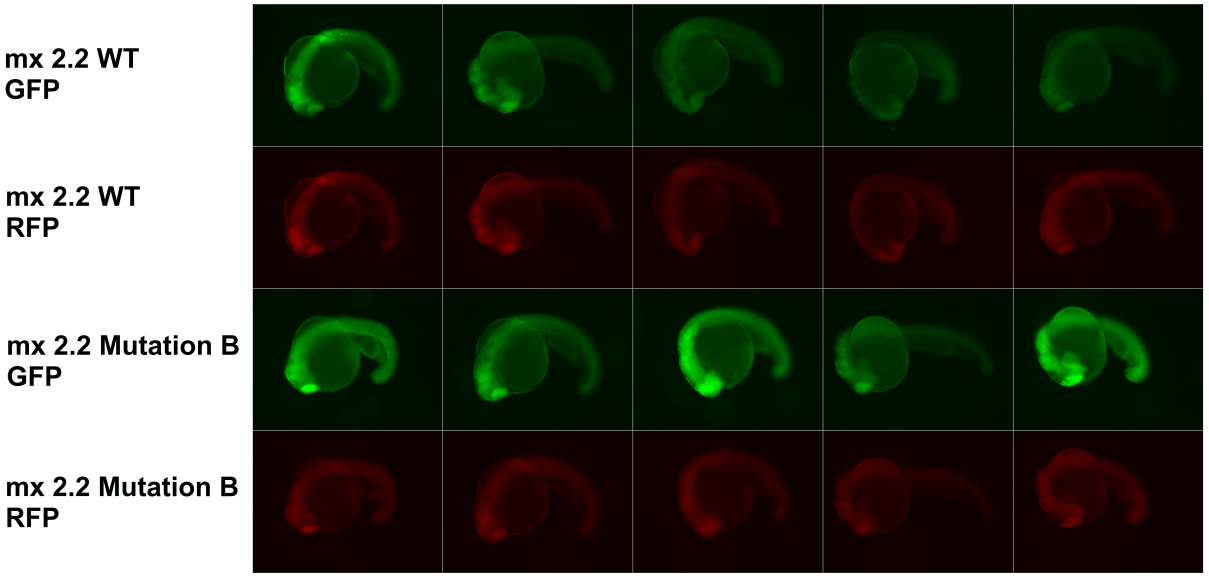

FIGURE 3.12: Images taken at 24 hpf of GFP and RFP fluorescence levels of zebrafish injected with mRNA with *mx2.2* WT and mutation B insert in their 3'UTR. Image shows 5 different individuals. Image shows 5 different individuals for the WT insert and 5 different individuals for the mutation B insert.

TABLE 3.5: Measured fluorescene levels from the first *mx2.2* experiment at 12, 24 and 48 hpf. Measured fluorescene has been refined and normalized against RFP fluorescence levels.

	12 hpf	24 hpf	48 hpf
mx2.2-WT 1	x	x	x
mx2.2-WT 2	29.25	x	x
mx2.2-WT 3	26.69	23.67	11.44
mx2.2-WT 4	26.63	26.03	12.85
mx2.2-WT 5	21.32	22.75	10.83
mx2.2-WT 6	23.64	26.20	x
mx2.2-Mut A 1	152.67	x	x
mx2.2-Mut A 2	65.09	56.41	24.60
mx2.2-Mut A 3	80.20	64.90	29.57
mx2.2-Mut A 4	78.44	81.29	44.12
mx2.2-Mut A 5	x	x	x
mx2.2-Mut A 6	x	x	x
mx2.2-Mut B 1	102.26	101.43	46.96
mx2.2-Mut B 2	33.38	34.70	19.82
mx2.2-Mut B 3	30.94	30.87	16.82
mx2.2-Mut B 4	92.68	97.96	51.11
mx2.2-Mut B 5	41.88	48.31	24.75
mx2.2-Mut B 6	81.96	88.19	45.49

Images of mutation B were taken 12, 24 and 48 hpf of embryos injected with mutation B 3'UTR insert of the *mx2.2* gene, figure 14. This figure shows a bigger difference in fluorescence intensity between the WT and the second mutation. Fluorescence values for the experiment with 18 individuals of mutant B were significant at 12 hpf ($p < 0.027$), at 24 hpf ($p < 0.037$) and at 48 hpf ($p < 0.0006$). Fluorescence values for the experiment with 6 individuals of mutant A were significant at 12 hpf ($p < 0.02$), at 24 hpf ($p < 0.01$) and at 48 hpf ($p < 0.04$). Fluorescence values for the experiment with 6 individuals of mutant B were significant at 12 hpf ($p < 0.02$), at 24 hpf ($p < 0.01$) and at 48 hpf ($p < 0.01$).

TABLE 3.6: Measured fluorescene levels from the second *mx2.2* experiment at 12, 24 and 48 hpf. Measured fluorescene has been refined and normalized against RFP fluorescence levels.

	12 hpf	24 hpf	48 hpf
mx2.2-WT 1	31.51	29.54	19.67
mx2.2-WT 2	x	x	x
mx2.2-WT 3	47.97	46.86	24.79
mx2.2-WT 4	51.90	50.91	24.37
mx2.2-WT 5	26.68	23.82	17.01
mx2.2-WT 6	25.37	38.47	21.72
mx2.2-WT 7	46.79	52.73	x
mx2.2-WT 8	46.10	45.87	18.60
mx2.2-WT 9	31.61	29.90	20.97
mx2.2-WT 10	29.76	30.04	20.90
mx2.2-WT 11	22.29	21.48	14.72
mx2.2-WT 12	60.86	63.17	33.58
mx2.2-WT 13	31.56	33.75	19.29
mx2.2-WT 14	27.20	29.10	16.31
mx2.2-WT 15	13.79	16.26	10.48
mx2.2-WT 16	46.79	53.24	x
mx2.2-WT 17	67.40	x	x
mx2.2-WT 18	58.08	55.88	25.04
mx2.2-Mut B 1	x	x	x
mx2.2-Mut B 2	x	x	x
mx2.2-Mut B 3	x	x	x
mx2.2-Mut B 4	64.74	x	x
mx2.2-Mut B 5	54.29	55.98	28.39
mx2.2-Mut B 6	25.02	26.51	x
mx2.2-Mut B 7	81.08	78.90	35.60
mx2.2-Mut B 8	40.72	42.89	24.60
mx2.2-Mut B 9	39.27	41.78	23.96
mx2.2-Mut B 10	77.79	75.42	36.77
mx2.2-Mut B 11	32.17	31.03	17.61
mx2.2-Mut B 12	x	x	x
mx2.2-Mut B 13	91.75	75.70	36.17
mx2.2-Mut B 14	68.05	63.31	32.51
mx2.2-Mut B 15	32.82	39.69	30.91
mx2.2-Mut B 16	77.58	68.41	37.21
mx2.2-Mut B 17	38.34	35.31	x
mx2.2-Mut B 18	26.77	26.87	x

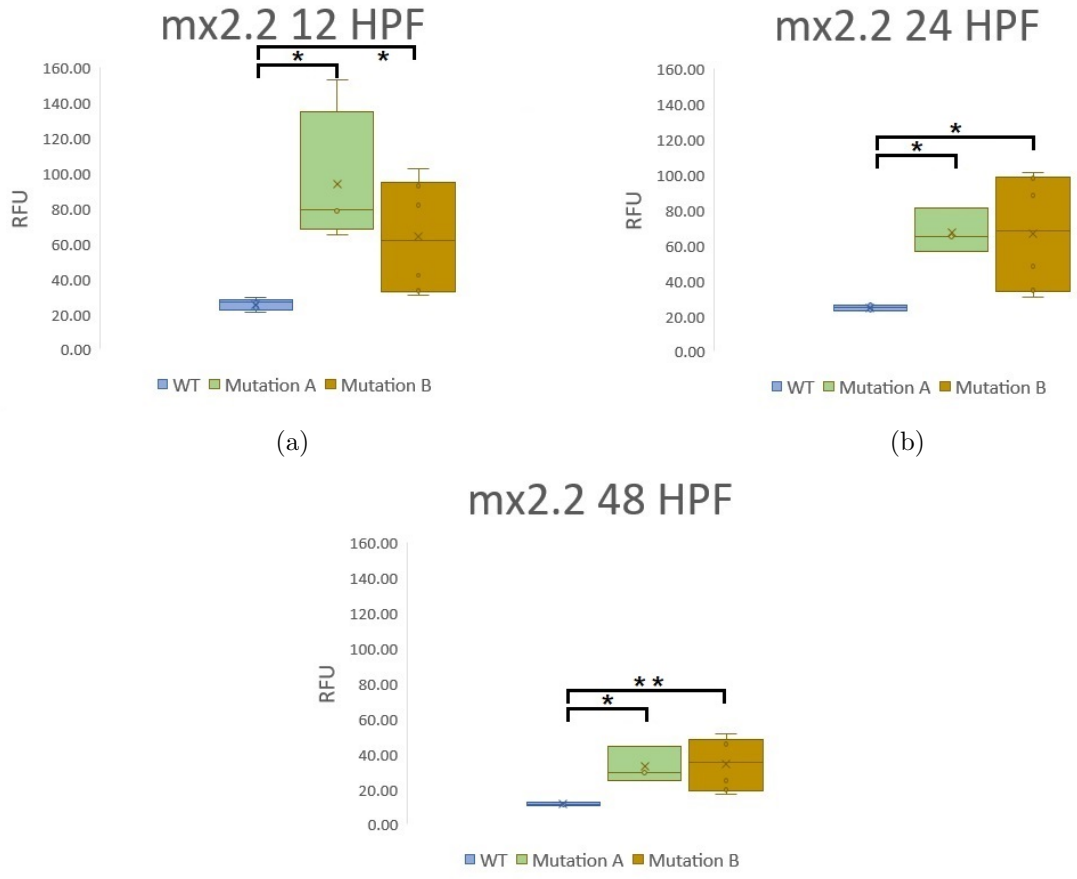

(a) (b)

(c)

FIGURE 3.13: Boxplots showing the difference of fluorescence levels of mRNA injected with the *mx2.2* WT insert and mutation A and B inserts. GFP fluorescence values has been normalized against RFP fluorescence values. a) Fluorescence levels at 12 hpf, b) fluorescence levels at 24 hpf and c) fluorescence levels at 48 hpf

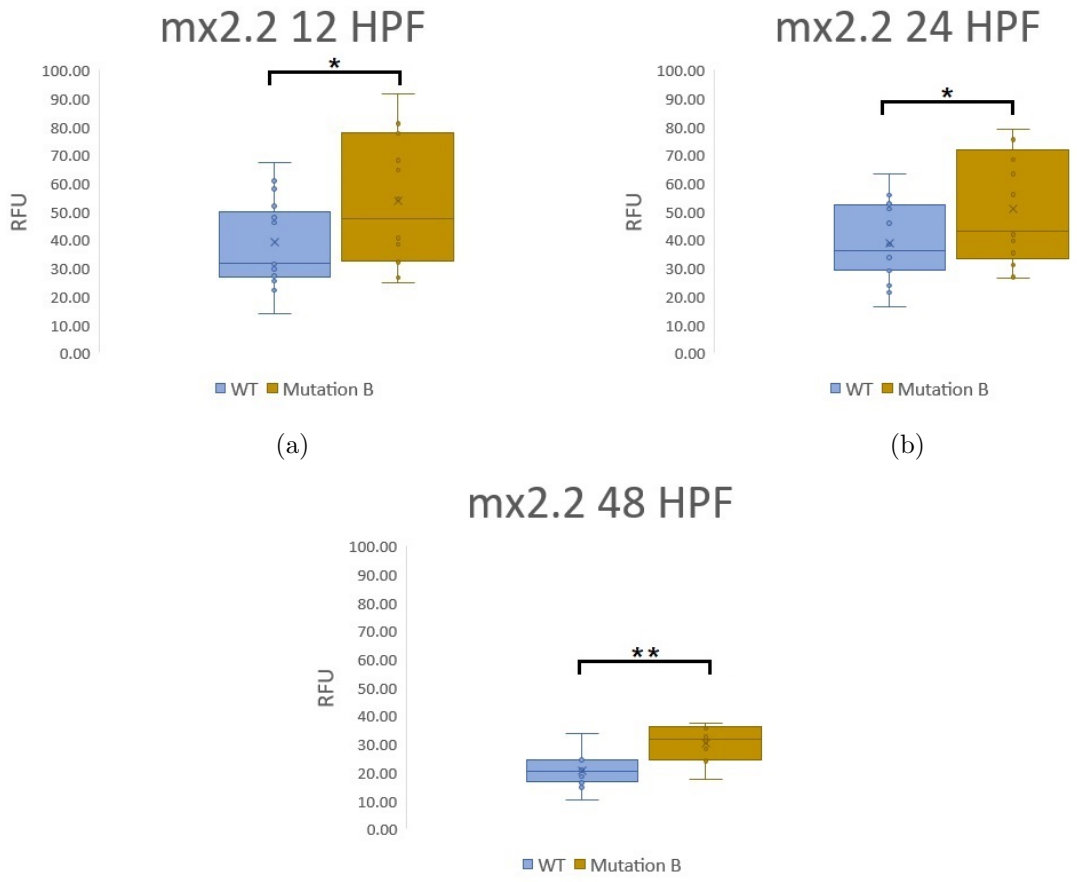

FIGURE 3.14: Boxplots showing the difference of fluorescence levels of mRNA injected with the *mx2.2* WT insert and mutation B insert. GFP fluorescence values has been normalized against RFP fluorescence values. a) Fluorescence levels at 12 hpf, b) fluorescence levels at 24 hpf and c) fluorescence levels at 48 hpf

Discussion

4.1 Discussion

In this study we explored approaches to assess zygotic mRNA stability by focusing on the role of the 3'UTR, which has been extensively studied [14]. We have applied different methodologies to assess the function of mRNA stability. Studies done by Vejnar et al. [16], Rabani et al. [17], and Yartseva et al. [47], demonstrates methods for identifying stabilizing and destabilizing elements in the 3'UTR. Vejnar et al. [16] successfully managed to show increased levels of GFP fluorescence in mutated 3'UTR sequences from the *trip10a* gene where de-stabilizing elements were mutated. In our study, we mutated the *trip10a* gene insert similarly to the way they mutated the insert (Figure 3.4). Mutating the insert in the same way as previously reported enabled us to implement method development on the assumption that our mutated insert would show an increase in GFP fluorescence. In addition to mutating the *trip10a* gene insert for method validation, our study focused on the two elements, ATTTA and AAATAAA, identified in the salmon *mx2.2* gene 3'UTR. In addition to mutating these two elements (mutation A), we also performed mutations in other sequences that contained AT repeats (Mutation B). Mutations in these AT repeats was not the main focus in our study, but we wanted to investigate if these AT repeats in the 3'UTR of the *mx2.2* gene (mutation B) had an effect on GFP fluorescence.

4.1.1 Selecting plasmid vectors

In order to assess regulatory elements in the 3'UTR we decided to use GFP reporter systems. Reporter systems based on GFP have been a widely used method in zebrafish research [48–51] with a diverse range of applications. GFP reporter systems have been used to assess mRNA stability in both cell cultures [52] and in zebrafish [16, 53]. The transposon Tol2 system [54–57] was evaluated to injecting the embryos with mRNA. Results from Tol2 injections showed high levels of fluorescence (Figure 3.1b), however we deemed it not suitable for comparison between individuals due to a very mosaic expression pattern and large variation within the tissue of injected individuals. Tol2 integrates randomly into the genome and the positions of the different integrations are affected by position effect variegation (PEV) [58]. The PEV therefore possibly affects expression levels of the GFP mRNA and leads to the observed variation. In addition to this, the Tol2 system exhibited higher levels of fluorescence in the yolk compared to the rest of the zebrafish body, leading to high levels of background noise. GFP fluorescence from injected mRNA was more consistent across individuals and more uniform across the body of each individual (Figures 3.1a and 3.1c). Embryos injected with mRNA also showed lower levels of fluorescence in the yolk. The lack of uniform GFP expression in individuals injected with the Tol2 vector lead us to discard the transposon Tol2 system in favour of injecting embryos with mRNA directly. In contrast to the incompatibility of the Tol2 system to our study, injections of mRNA directly into the embryo were more in line with the overall goals of the study. Injecting mRNA to study mRNA stability seemed a more logical approach to test 3'UTR regulatory elements, whereas the Tol2 vector also would include transcription of the intended vector as a source of variation. The two remaining plasmid vectors, pCS2 GFP and pUCIDT (Figures 2.2a and 2.2e), were tested further. The pCS2 GFP and pUCIDT plasmid vectors performed similarly in initial testing, however pCS2 GFP was chosen to be able to directly compare our results with a similar published study [16] with the same vector system.

4.1.2 Effect of 3'UTR AREs on mRNA stability

4.1.2.1 Mutations in 3'UTR AREs increases *trip10a* mRNA stability

Two established AREs from the *trip10a* 3'UTR, AAATAAA and ATTTA, were disrupted by mutations (Figure 3.4). In addition to this, one possible ARE, AAATAA, was disrupted as well as 6 TA sequences. In the middle of the insert another sequence, AAGCGCTT, is a sequence proposed to be a miR-430 target site [16]. This potential microRNA target site was also disrupted, but it is likely that the disruption of this sequence had little to no effect on mRNA stability in this study as it has been shown to have no effect in a previous study [16].

Results from the two *trip10a* injection-experiments shows a significant increase of GFP fluorescence levels in individuals injected with the mutated version of the *trip10a* insert compared with individuals injected with the *trip10a* WT insert (Figures 3.8 and 3.9). In accordance with the primary aim of this thesis, our method gave statistically significant and reproducible results and can be used as a robust method for measuring mRNA stability.

4.1.2.2 Embryo lethality in the *trip10a* experiments

The first injection-experiment had 18 sample individuals, while the other experiment had 6 sample individuals, both for the WT insert and the mutated insert (Tables 3.4 and 3.3). In the first experiment, samples were collected and imaged at 24, 48, 72, 96, and 120 hpf. At 24 hpf 16 individuals had survived and were tested for *trip10a* WT and 4 out of those 16 survived to 120 hpf. For the mutated *trip10a* insert, 14 individuals were alive at 24 hpf and 11 survived all the way to 120 hpf. In the second experiment, samples were collected and imaged at 6, 12, and 24 hpf. All individuals survived in the second experiment, except one individual which did not survive after 12 hpf. Zebrafish injected with mRNA with the *trip10a* 3'UTR insert showed a high mortality rate, particularly from individuals

injected with the WT insert. At 48 hpf, 75 % of the individuals sampled at 24 hpf were dead. Mortality rate for individuals injected with the mutated insert were lower, about 20 % of the individuals died between 24 and 48 hpf. The reason for the high mortality rates seen in the *trip10a* WT is unknown. The process of injecting the zebrafish, and later incubating them for 5 days, and imaging every 24 hours included certain factors that might have contributed to high mortality rates. The zebrafish were dechorionated prior to imaging at 24 hpf. dechorionation was performed manually by puncturing the chorion with a needle, and then pulling the deflated chorion apart with a pair of forceps to make a hole big enough for the embryo. During this process the embryos might have been damaged, either by unintentional rupture of tissues inflicted by the needle or forceps, or by the hole in the embryo being too small for the delicate embryo, thus compressing it too much on the way out. Handling the embryos after dechorionation via pipette for transportation to and from Petri dishes for imaging and incubation might have damaged the embryos.

4.1.2.3 Visual analysis of GFP fluorescence of *trip10a* 3'UTR mRNA elements

Results from two *trip10a* injection-experiments were comparable with results from a previous study [16]. We observed an increase in GFP fluorescence levels for the mutant compared to the WT sequence. Several images were taken throughout this study during testing and optimization of the method, and it was apparent that the images taken of the mutated version of the *trip10a* gene 3'UTR insert consistently showed a stronger fluorescence. As seen in figures 3.5, 3.7 and 3.6, there is a visually distinct difference in fluorescence in the two inserted sequences. From the initial imaging of embryos injected with mRNA with the *trip10a* insert, both the WT and mutated, we observed that GFP fluorescence levels at 48, 72, 96 and 120 hpf were comparatively lower than for 24 hpf (Figure 3.5). Based on this observation, images of zebrafish embryos were taken earlier than 24 hpf. Images taken at 6, 12 and 24 hpf (Figure 3.6) showed strong and consistent levels of GFP fluorescence for injected mRNA with the mutated insert for all the three

time points. Based on the observation that GFP fluorescence levels were strongest at and prior to 24 hpf, we decided that images of embryos injected with mRNA containing the *mx2.2* inserts would be imaged at 12, 24 and 48 hpf.

4.1.2.4 Mutations in Atlantic salmon *mx2.2* 3'UTR AREs increases mRNA stability

Based on observations from the *trip10a* injection-experiments and proposed regulatory elements from Vejnar et al. [16], we located a stretch in the 3'UTR of the *mx2.2* gene containing two putative AREs, AAATAAA and ATTTA. The two AREs in the *mx2.2* 3'UTR insert, AAATAAA and ATTTA, were disrupted by 8 mutations, 4 mutations in each ARE. These 8 mutations were done for both mutation A and mutation B (Figure 3.4). In addition to mutating these AREs, mutation B were mutated further by disrupting AT and TA sequences. In total 12 mutations were done in select TA sequences throughout the insert.

Results from the two *mx2.2* injection-experiments shows a significant increase of GFP fluorescence levels in individuals injected with the mutated version of the *mx2.2* insert compared with individuals injected with the *mx2.2* WT insert (Figures 3.13 and 3.14). Image analysis from both experiments showed significant results, and disrupting AREs in the salmon *mx2.2* gene appear to have increased mRNA stability. We predicted to observe a difference in GFP fluorescence by mutating the two putative AREs, AAATAAA and ATTTA. The results show an increase in GFP fluorescence by mutating these AREs, however the visual difference in fluorescence is not as apparent for the *mx2.2* injection-experiments as it were for the *trip10a* injection-experiments (Figures 3.7, 3.11 and 3.12).

4.1.2.5 Embryo lethality in the *mx2.2* experiments

Two injection-experiments were performed to assess the effect of 3'UTR ARE on mRNA stability in mRNA with the insert from the *mx2.2* gene, similarly to inserts from the

trip10a gene. One experiment had 18 sample individuals with the WT insert and 18 sample individuals with the mutation B insert, and the other experiment had 6 sample individuals with the WT insert, 6 sample individuals with the mutation A insert, and 6 sample individuals with the mutation B insert (Tables 3.6 and 3.5). In total 17 individuals were tested for *mx2.2* WT, 14 were tested for the mutation B. 14 individuals survived all the way to 48 hpf. From the Mutation 10 individuals survived all the way to 120 hpf (Table 3.4). In the experiment with both mutation A and mutation B 5 out of 6 individuals survived 12 hpf for WT, 4 out of 5 for mutation A and all survived all the time for mutation B.

4.1.2.6 Visual analysis of GFP fluorescence of *mx2.2* 3'UTR mRNA elements

Based on previous observations of GFP expression from the *trip10a* insert experiments where GFP fluorescence was considerably lower post 24 hpf (Figures 3.5 and 3.6), samples of individuals with the *mx2.2* insert were imaged at 12, 24, and 48 hpf.

Images from our experiments on the inserts from the *mx2.2* suggests that there is a visually detectable difference between the WT insert and both mutated versions of the insert (Mutation A and B)(Figures 3.10, 3.11 and 3.12). There is no apparent visual difference between mutation A and mutation B, and image analysis confirms this (Figure 3.13). This observation might indicate that the additional mutations done in mutation B in disrupting AT and TA sequences, had little to no effect on mRNA stability. The effect on GFP fluorescence seen between the WT insert and the mutations might thus be caused by mutations done to the two AREs ATTTA and AAATAAA found in the 3'UTR of the *mx2.2* gene.

It is also apparent that GFP fluorescence for the *mx2.2* WT insert is high to begin with compared with the GFP fluorescence from the *trip10a* WT insert. This difference between fluorescence levels using *trip10a*, and *mx2.2* WT inserts might be due to the *trip10a* WT insert containing more potential AREs. The *trip10a* WT insert contains two

defined AREs, AAATAAA and ATTTA, but in addition to these the insert contained one additional possible ARE, AAATAA. The *trip10a* WT insert also contained on average, more A and T nucleotides in different configurations. There might be reason to believe that the presence of more As and Ts would contribute to destabilize the 3'UTR further. In the *mx2.2* WT insert, only two regions were defined as AREs, ATTTA and AAATAAA. In *mx2.2* mutation A these two sequences were disrupted by 8 mutations, 4 mutations in each ARE. In *mx2.2* mutation B additional 12 mutations were introduced to disrupt TA and AT sequences in the insert (Figure 3.4).

4.1.3 Methodological considerations

4.1.3.1 Sampling and microinjection

The amount of embryos injected outweighed the amount of embryos that were subsequently selected for imaging. 18 and 6 embryos were sampled for each insert for both *trip10a* and *mx2.2* experiments. Embryos were not screened for GFP at this stage to avoid bias in the sampling. Sampling was based on selecting embryos which had visually similar RFP fluorescence, for to subsequently normalize GFP fluorescence.

Microinjection of zebrafish also has its challenges. The injection system is based on injections from a pressure system. Amount of injected mRNA is based on a fixed pressure, not a fixed volume. There might be inconsistencies behind the pressure and flowback into the needle could occur. Also zebrafish eggs vary in size. This size variation might be miniscule, but it is there. The ruler was implemented to reduce the impact of these uncertainties. Also, approximately 200 eggs were injected in each session. Mortality from injections might play a factor here. Some eggs died the same day, however some embryos died the next day and some at 48 hpf. If embryos survived to 48 hpf, they usually survived all the way to 120 hpf.

4.1.3.2 Image analysis and quantification

All embryos were imaged under the same conditions, 1 second exposure time and 1,0 gain unless noted otherwise. Embryos at 6 and 12 hpf are a sphere consisting mainly of the yolk and a cellular mass enveloping the yolk. Orienting the embryos under the microscope, with and without chorion, to focus on the cells rather than the yolk provided a challenge. Extreme care was exercised to prevent either the chorion from deflating, or the dechorionated embryos from rupturing. At 24 hpf the embryos morphology had developed to a point where it was possible to orient them consistently and accurately, however at this stage the yolk was still large. The orientation of the yolk would sometimes obscure tissue or align the embryo at an awkward angle. Manual repositioning of the embryos solved this and enabled for consistent and accurate imaging. Mounting the embryos in a viscous solution prior to imaging was considered. This would result in improved control over embryo orientation and might have improved image quality. However, multiple images were taken during the work on this thesis, and each embryo was imaged several times during development. Embryos might not survive the mounting process and the practical benefits of being able to image several embryos in short succession outweighed the possible gain in image quality by mounting.

Statistical analysis of measured GFP fluorescence levels was performed by first removing background noise observed in the ImageJ software (Figures 2.6b and 2.6c). Mean values for both GFP and RFP fluorescence were then subtracted from the values acquired from ImageJ (Tables 3.1 and 3.2). Mean refined RFP fluorescence values were standardized for each time point; 6, 12, 24, 48, 72, 96, and 120 hpf, and the refined GFP fluorescence values were normalized against the mean refined RFP fluorescence values. During this process some mathematical artefacts emerged, such as GFP fluorescence values exhibiting negative values (Table 3.4). These negative values are a result of natural variability of actual RFP fluorescence in the samples, and the fact that GFP fluorescence for the *trip10a* WT insert after 24 hpf were low. In two instances GFP fluorescence values showed high negative values for *trip10a*-WT 1 and *trip10a*-Mut 8 individuals (Table

3.4). RFP fluorescence for these two individuals were substantially lower than expected, and normalization of the values skewed GFP fluorescence to such an extent that they have been removed as data points. It is apparent that there is a distinct difference of statistical significance between the *trip10a* and *mx2.2* experiments. Results from the *trip10a* experiments are more confident than that of the *mx2.2* experiment. However, both experiments show a significant increase in GFP fluorescence for the mutated inserts over the WT inserts, indicating that the mutated sequences provide increased mRNA stability.

4.1.4 Alternative methods

4.1.4.1 QPCR

Other possible ways of assessing mRNA stability would be by using qPCR [59]. A qPCR analysis would provide measurements of how much RNA was present in the sample. This would have been a more direct indication of mRNA longevity, rather than measuring GFP fluorescence levels. However, for robust qPCR a larger number of individuals are required to obtain sufficient amounts of RNA per reaction. We have performed pilot tests (per.com, unpublished results, Raudstein), but the preliminary results were so far inconclusive. qPCR analysis will be more reasonable to do on Atlantic salmon, seeing that a lower number of individual samples for salmon are needed to obtain enough RNA for each reaction.

4.1.4.2 Plate reader

A Tecan Spark multimode plate reader (Tecan Trading AG, Switzerland) was tested as a possible method for quantification of GFP fluorescence. Plate reader analysis was performed by putting zebrafish embryos in a 96-well micro-plate which would in turn measure fluorescence levels of the embryos in the well [60]. Plate reader required a lot of

individuals and the manual work load was intensive. There were also issues concerning the accuracy of the measured fluorescence, as it was difficult to consistently orient the embryos comparatively in the wells. Because of these limitations we discontinued our trails with the plate reader and rather used the ImageJ approach.

4.1.5 Method transferability to Atlantic salmon

The method described in this study could be applied for Salmon directly. The plan is to inject the same mRNA with inserts from both *trip10a* and *mx2.2* that was used in this thesis to see whether comparable results would be obtained in Salmon. However, Salmon has a longer developmental time and take about 3 months before hatching. Thus the GFP expression from injected mRNA might have to be analysed earlier in the development, before hatching due to the mRNA half-life. Preliminary testing would have to be done to assess at what time during development the injected mRNA with a WT insert would degrade. It might be interesting to investigate whether RNA-Binding Proteins (RBPs) associated with mRNA stability have similarities in peptide sequences between zebrafish and Salmon. If the mechanisms of mRNA stability concerning ARE and RBPs are conserved mechanisms across species, it would be possible to use this method to make general predictions of its applicability.

4.2 Conclusion

In this study we demonstrate a robust and efficient method for assessing mRNA stability using zebrafish as a model organism. Experiments with the 60 bp insert from the *trip10a* 3'UTR show a significant increase of GFP fluorescence when mutations were made to disrupt AREs in the 3'UTR. Although this study presents results from disrupting AREs, I predict that this method can be used successfully in testing other regulatory elements found in the 3'UTR, such as disrupting microRNA sites.

Experiments done in this study also demonstrate a significant increase in fluorescence of GFP by making mutations to disrupt AREs in the 3'UTR of the salmon gene *mx2.2*. This indicates that AREs in *mx2.2* can be modulated to increase mRNA stability, but further in vivo studies are needed to confirm whether the results obtained using zebrafish are reproducible in Atlantic salmon.

4.3 Future perspectives

This thesis presents a method for assessing the influence of 3'UTR regulatory elements on mRNA stability. The TUNESAL project, which this thesis is a part of, is currently optimizing and fine tuning the CRISPR/Cas9 technology to make precise edits in the Salmon genome. Results from this thesis will aid in future work to identify salmon elements which can be altered to increase the stability of transcripts to modulate protein levels in salmon, to possibly make salmon more robust and more resistant to diseases. This would lead to better fish welfare in aquaculture production. Also other important traits important for a more sustainable aquaculture can be improved using this technology and should be a topic for future studies. This technology, in combination with sterile fish so that gene-edited salmon cannot spread the altered genome to the wild populations, might contribute to a more robust and sustainable salmon aquaculture.

References

[1] Arnau Sebé-Pedrós, Cecilia Ballaré, Helena Parra-Acero, Cristina Chiva, Juan J. Tena, Eduard Sabidó, José Luis Gómez-Skarmeta, Luciano Di Croce, and Iñaki Ruiz-Trillo. The Dynamic Regulatory Genome of Capsaspora and the Origin of Animal Multicellularity. *Cell*, 165(5):1224–1237, may 2016. ISSN 0092-8674. doi: 10.1016/J.CELL.2016.03.034.

[2] Vicky W. Zhou, Alon Goren, and Bradley E. Bernstein. Charting histone modifications and the functional organization of mammalian genomes. *Nature reviews. Genetics*, 12(1):7–18, jan 2011. ISSN 1471-0064. doi: 10.1038/NRG2905.

[3] Guohua Wang, Fang Wang, Qian Huang, Yu Li, Yunlong Liu, and Yadong Wang. Understanding Transcription Factor Regulation by Integrating Gene Expression and DNase I Hypersensitive Sites. *BioMed Research International*, 2015, 2015. ISSN 23146141. doi: 10.1155/2015/757530.

[4] Qun Pan, Ofer Shai, Leo J. Lee, Brendan J. Frey, and Benjamin J. Blencowe. Deep surveying of alternative splicing complexity in the human transcriptome by high-throughput sequencing. *Nature Genetics 2008 40:12*, 40(12):1413–1415, nov 2008. ISSN 1546-1718. doi: 10.1038/ng.259.

[5] Shai S. Shen-Orr, Yitzhak Pilpel, and Craig P. Hunter. Composition and regulation of maternal and zygotic transcriptomes reflects species-specific reproductive mode. *Genome Biology*, 11(6):1–13, jun 2010. ISSN 14747596. doi: 10.1186/GB-2010-11-6-R58/FIGURES/4.

[6] Alexander F. Schier. The maternal-zygotic transition: Death and birth of RNAs. *Science*, 316(5823):406–407, apr 2007. ISSN 00368075. doi: 10.1126/SCIENCE.1140693/ASSET/DA3B4BF6-729D-49D7-B6FE-788E7F986CC4/ASSETS/GRAPHIC/316_406_F1.JPEG.

[7] Antonio J. Giraldez, Yuichiro Mishima, Jason Rihel, Russell J. Grocock, Stijn Van Dongen, Kunio Inoue, Anton J. Enright, and Alexander F. Schier. Zebrafish MiR-430 promotes deadenylation and clearance of maternal mRNAs. *Science (New York, N.Y.)*, 312(5770):75–79, apr 2006. ISSN 1095-9203. doi: 10.1126/SCIENCE.1122689.

[8] Karoline Holler, Anika Neuschulz, Philipp Drewe-Boß, Janita Mintcheva, Bastiaan Spanjaard, Roberto Arsiè, Uwe Ohler, Markus Landthaler, and Jan Philipp Junker. Spatio-temporal mRNA tracking in the early zebrafish embryo. *Nature Communications 2021 12:1*, 12(1):1–13, jun 2021. ISSN 2041-1723. doi: 10.1038/s41467-021-23834-1.

[9] Patricia Heyn, Martin Kircher, Andreas Dahl, Janet Kelso, Pavel Tomancak, Alex T. Kalinka, and Karla M. Neugebauer. The Earliest Transcribed Zygotic Genes Are Short, Newly Evolved, and Different across Species. *Cell Reports*, 6(2):285–292, jan 2014. ISSN 2211-1247. doi: 10.1016/J.CELREP.2013.12.030.

[10] Aude Trinquier, Sylvain Durand, Frédérique Braun, and Ciarán Condon. Regulation of RNA processing and degradation in bacteria. *Biochimica et Biophysica Acta (BBA) - Gene Regulatory Mechanisms*, 1863(5):194505, may 2020. ISSN 1874-9399. doi: 10.1016/J.BBAGRM.2020.194505.

[11] Hélène Tourrière, Karim Chebli, and Jamal Tazi. mRNA degradation machines in eukaryotic cells. *Biochimie*, 84(8):821–837, aug 2002. ISSN 0300-9084. doi: 10.1016/S0300-9084(02)01445-1.

[12] Edward Yang, Erik van Nimwegen, Mihaela Zavolan, Nikolaus Rajewsky, Mark Schroeder, Marcelo Magnasco, and James E. Darnell. Decay Rates of Human mRNAs: Correlation With Functional Characteristics and Sequence Attributes. *Genome Research*, 13(8):1863, aug 2003. ISSN 10889051. doi: 10.1101/GR.1272403.

[13] Longfei Jia, Yuanhui Mao, Quanquan Ji, Devin Dersh, Jonathan W. Yewdell, and Shu Bing Qian. Decoding mRNA translatability and stability from the 5‘ UTR. *Nature Structural & Molecular Biology 2020 27:9*, 27(9):814–821, jul 2020. ISSN 1545-9985. doi: 10.1038/s41594-020-0465-x.

[14] Christine Mayr. Regulation by 3‘-Untranslated Regions. *Annual Review of Genetics*, 51(1):171–194, nov 2017. ISSN 0066-4197. doi: 10.1146/annurev-genet-120116-024704.

[15] David A. Siegel, Olivier Le Tonqueze, Anne Biton, Noah Zaitlen, and David J. Erle. Massively Parallel Analysis of Human 3‘UTRs Reveals that AU-Rich Element Length and Registration Predict mRNA Destabilization. *bioRxiv*, page 2020.02.12.945063, feb 2020. doi: 10.1101/2020.02.12.945063.

[16] Charles E. Vejnar, Mario Abdel Messih, Carter M. Takacs, Valeria Yartseva, Panos Oikonomou, Romain Christiano, Marlon Stoeckius, Stephanie Lau, Miler T. Lee, Jean Denis Beaudoin, Damir Musaev, Hiba Darwich-Codore, Tobias C. Walther, Saeed Tavazoie, Daniel Cifuentes, and Antonio J. Giraldez. Genome wide analysis of 3‘UTR sequence elements and proteins regulating mRNA stability during maternal-to-zygotic transition in zebrafish. *Genome Research*, 29(7):1100–1114, 2019. ISSN 15495469. doi: 10.1101/gr.245159.118.

[17] Michal Rabani, Lindsey Pieper, Guo Liang Chew, and Alexander F. Schier. A Massively Parallel Reporter Assay of 3'UTR Sequences Identifies In Vivo Rules for mRNA Degradation. *Molecular Cell*, 68(6):1083–1094.e5, 2017. ISSN 10974164. doi: 10.1016/j.molcel.2017.11.014.

[18] Chyi Ying A. Chen and Ann Bin Shyu. AU-rich elements: characterization and importance in mRNA degradation. *Trends in biochemical sciences*, 20(11):465–470, 1995. ISSN 0968-0004. doi: 10.1016/S0968-0004(00)89102-1.

[19] Sofía M. García-Mauriño, Francisco Rivero-Rodríguez, Alejandro Velázquez-Cruz, Marian Hernández-Vellisca, Antonio Díaz-Quintana, Miguel A. De la Rosa, and Irene Díaz-Moreno. RNA binding protein regulation and cross-talk in the control of AU-rich mRNA Fate. *Frontiers in Molecular Biosciences*, 4(OCT):71, oct 2017. ISSN 2296889X. doi: 10.3389/FMOLB.2017.00071/BIBTEX.

[20] Hiroshi Otsuka, Akira Fukao, Yoshinori Funakami, Kent E. Duncan, and Toshinobu Fujiwara. Emerging evidence of translational control by AU-rich element-binding proteins. *Frontiers in Genetics*, 10(MAY):332, 2019. ISSN 16648021. doi: 10.3389/FGENE.2019.00332/BIBTEX.

[21] Robert L Tanguay and Daniel R Gallie. Translational efficiency is regulated by the length of the 3' untranslated region. *Molecular and Cellular Biology*, 16(1):146, jan 1996. ISSN 0270-7306. doi: 10.1128/MCB.16.1.146.

[22] Marc Robert Fabian, Nahum Sonenberg, and Witold Filipowicz. Regulation of mRNA Translation and Stability by microRNAs. *Annual Review of Biochemistry*, 79:351–379, 2010. doi: 10.1146/annurev-biochem-060308-103103.

[23] Statistics Norway. Aquaculture. Technical report, 2017.

[24] Geir Lasse Taranger, Ørjan Karlsen, Raymond John Bannister, Kevin Alan Glover, Vivian Husa, Egil Karlsbakk, Bjørn Olav Kvamme, Karin Kroon Boxaspen, Pål Arne Bjørn, Bengt Finstad, Abdullah Sami Madhun, H. Craig Morton, and Terje Svåsand. Risk assessment of the environmental impact of Norwegian Atlantic salmon farming. *ICES Journal of Marine Science*, 72(3):997–1021, mar 2015. ISSN 1054-3139. doi: 10.1093/ICESJMS/FSU132.

[25] Norwegian Veterinary Institute. The Fish Health Report. Technical report, 2020.

[26] A. J.A. McBeath, M. Snow, C. J. Secombes, A. E. Ellis, and B. Collet. Expression kinetics of interferon and interferon-induced genes in Atlantic salmon (Salmo salar) following infection with infectious pancreatic necrosis virus and infectious salmon anaemia virus. *Fish & shellfish immunology*, 22(3):230–241, 2007. ISSN 1050-4648. doi: 10.1016/J.FSI.2006.05.004.

[27] Aase B. Mikalsen, Oyvind Haugland, Marit Rode, Inge Tom Solbakk, and Oystein Evensen. Atlantic Salmon Reovirus Infection Causes a CD8 T Cell Myocarditis in

Atlantic Salmon (Salmo salar L.). *PLOS ONE*, 7(6):e37269, jun 2012. ISSN 1932-6203. doi: 10.1371/JOURNAL.PONE.0037269.

[28] Gerrit Timmerhaus, Aleksei Krasnov, Pål Nilsen, Marta Alarcon, Sergey Afanasyev, Marit Rode, Harald Takle, and Sven M. Jørgensen. Transcriptome profiling of immune responses to cardiomyopathy syndrome (CMS) in Atlantic salmon. *BMC Genomics*, 12(1):1–17, sep 2011. ISSN 14712164. doi: 10.1186/1471-2164-12-459/TABLES/1.

[29] Søren Grove, Lars Austbø, Kjartan Hodneland, Petter Frost, Marie Løvoll, Marian McLoughlin, Hanna L. Thim, Stine Braaen, Melanie König, Mohasina Syed, Jorunn B. Jørgensen, and Espen Rimstad. Immune parameters correlating with reduced susceptibility to pancreas disease in experimentally challenged Atlantic salmon (Salmo salar). *Fish & shellfish immunology*, 34(3):789–798, 2013. ISSN 1095-9947. doi: 10.1016/J.FSI.2012.12.014.

[30] Erik Kjærner-Semb, Fernando Ayllon, Tomasz Furmanek, Vidar Wennevik, Geir Dahle, Eero Niemelä, Mikhail Ozerov, Juha Pekka Vähä, Kevin A. Glover, Carl J. Rubin, Anna Wargelius, and Rolf B. Edvardsen. Atlantic salmon populations reveal adaptive divergence of immune related genes - A duplicated genome under selection. *BMC Genomics*, 17(1):1–12, aug 2016. ISSN 14712164. doi: 10.1186/S12864-016-2867-Z/FIGURES/4.

[31] Anne Hege Straume, Erik Kjærner-Semb, Kai Ove Skaftnesmo, Hilal Güralp, Lene Kleppe, Anna Wargelius, and Rolf Brudvik Edvardsen. Indel locations are determined by template polarity in highly efficient in vivo CRISPR/Cas9-mediated HDR in Atlantic salmon. *Scientific Reports 2020 10:1*, 10(1):1–9, jan 2020. ISSN 2045-2322. doi: 10.1038/s41598-019-57295-w.

[32] Anne Hege Straume, Erik Kjærner-Semb, Kai Ove Skaftnesmo, Hilal Güralp, Simon Lillico, Anna Wargelius, and Rolf Brudvik Edvardsen. Single nucleotide replacement in the Atlantic salmon genome using CRISPR/Cas9 and asymmetrical oligonucleotide donors. *BMC Genomics*, 22(1):1–8, dec 2021. ISSN 14712164. doi: 10.1186/S12864-021-07823-8/FIGURES/4.

[33] George Streisinger, Charline Walker, Nancy Dower, Donna Knauber, and Fred Singer. Production of clones of homozygous diploid zebra fish (Brachydanio rerio) Production of homozygous diploids. *Nature*, 291, 1981.

[34] Rowena Spence, Gabriele Gerlach, Christian Lawrence, and Carl Smith. The behaviour and ecology of the zebrafish, Danio rerio. *Biol. Rev*, 83(13):13–34, 2008. doi: 10.1111/j.1469-185X.2007.00030.x.

[35] Charles B Kimmel, William W Ballard, Seth R Kimmel, Bonnie Ullmann, and Thomas F Schilling. Stages of Embryonic Development of the Zebrafish. *Developmental Dynamics*, (203):253–310, 1995.

[36] Kimberly Dooley and Leonard I. Zon. Zebrafish: a model system for the study of human disease. *Current opinion in genetics & development*, 10(3):252–256, jun 2000. ISSN 0959-437X. doi: 10.1016/S0959-437X(00)00074-5.

[37] Graham J. Lieschke and Peter D. Currie. Animal models of human disease: zebrafish swim into view. *Nature Reviews Genetics 2007 8:5*, 8(5):353–367, may 2007. ISSN 1471-0064. doi: 10.1038/nrg2091.

[38] Yvonne M. Bradford, Sabrina Toro, Sridhar Ramachandran, Leyla Ruzicka, Douglas G. Howe, Anne Eagle, Patrick Kalita, Ryan Martin, Sierra A.Taylor Moxon, Kevin Schaper, and Monte Westerfield. Zebrafish Models of Human Disease: Gaining Insight into Human Disease at ZFIN. *ILAR Journal*, 58(1):4, jul 2017. ISSN 19306180. doi: 10.1093/ILAR/ILW040.

[39] Marta Carnovali, Giuseppe Banfi, and Massimo Mariotti. Zebrafish Models of Human Skeletal Disorders: Embryo and Adult Swimming Together. *BioMed Research International*, 2019, 2019. ISSN 23146141. doi: 10.1155/2019/1253710.

[40] Con Sullivan and Carol H. Kim. Zebrafish as a model for infectious disease and immune function. *Fish & Shellfish Immunology*, 25(4):341–350, oct 2008. ISSN 1050-4648. doi: 10.1016/J.FSI.2008.05.005.

[41] John Postlethwait, Angel Amores, Man Force, and Yi-Lin Yan. The Zebrafish Genome. *Methods in cell biology*, 60, 1999.

[42] Kerstin Howe, Matthew D. Clark, Carlos F. Torroja, James Torrance, Camille Berthelot, Matthieu Muffato, John E. Collins, Sean Humphray, and Et Al. The zebrafish reference genome sequence and its relationship to the human genome. *Nature 2013 496:7446*, 496(7446):498–503, apr 2013. ISSN 1476-4687. doi: 10.1038/nature12111.

[43] Greta Carmona-Antoñanzas, Xiaozhong Zheng, Douglas R. Tocher, and Michael J. Leaver. Regulatory divergence of homeologous Atlantic salmon elovl5 genes following the salmonid-specific whole-genome duplication. *Gene*, 591(1):34–42, oct 2016. ISSN 0378-1119. doi: 10.1016/J.GENE.2016.06.056.

[44] Ralf Dahm and Robert Geisler. Learning from small fry: The zebrafish as a genetic model organism for aquaculture fish species. *Marine Biotechnology*, 8(4):329–345, aug 2006. ISSN 14362228. doi: 10.1007/S10126-006-5139-0/FIGURES/5.

[45] Daniel G. Gibson, Lei Young, Ray Yuan Chuang, J. Craig Venter, Clyde A. Hutchison, and Hamilton O. Smith. Enzymatic assembly of DNA molecules up to several hundred kilobases. *Nature Methods*, 6(5):343–345, 2009. ISSN 15487091. doi: 10.1038/nmeth.1318.

[46] Gianluca D'Agati, Rosanna Beltre, Anna Sessa, Alexa Burger, Yi Zhou, Christian Mosimann, and Richard M. White. A defect in the mitochondrial protein mpv17 underlies the transparent casper zebrafish. *Developmental biology*, 430(1):11, oct 2017. ISSN 1095564X. doi: 10.1016/J.YDBIO.2017.07.017.

[47] Valeria Yartseva, Carter M. Takacs, Charles E. Vejnar, Miler T. Lee, and Antonio J. Giraldez. RESA identifies mRNA-regulatory sequences at high resolution. *Nature Methods*, 14(2):201–207, feb 2017. ISSN 15487105. doi: 10.1038/nmeth.4121.

[48] Ji Liao, Tie Yan, Choy L Hew, Toong Jin Lam, and Zhiyuan Gong. Faithful Expression of Green Fluorescent Protein (GFP) in Transgenic Zebrafish Embryos Under Control of Zebrafish Gene Promoters. *Dev. Genet*, 25:158–167, 1999.

[49] Yanwei Xi, Man Yu, Rafael Godoy, Gary Hatch, Luc Poitras, and Marc Ekker. Transgenic zebrafish expressing green fluorescent protein in dopaminergic neurons of the ventral diencephalon. *Developmental Dynamics*, 240(11):2539–2547, nov 2011. ISSN 1097-0177. doi: 10.1002/DVDY.22742.

[50] Zhiqiang Zeng, Xingjun Liu, Shalin Seebah, and Zhiyuan Gong. Faithful expression of living color reporter genes in transgenic medaka under two tissue-specific zebrafish promoters. *Developmental Dynamics*, 234(2):387–392, oct 2005. ISSN 10588388. doi: 10.1002/dvdy.20491.

[51] Chong Pyo Choe, Seok-Yong Choi, Yun Kee, Min Jung Kim, Seok-Hyung Kim, Yoonsung Lee, Hae-Chul Park, and Hyunju Ro. Transgenic fluorescent zebrafish lines that have revolutionized biomedical research. *Laboratory Animal Research 2021 37:1*, 37(1):1–29, sep 2021. ISSN 2233-7660. doi: 10.1186/S42826-021-00103-2.

[52] Don Benjamin, Marco Colombi, Georg Stoecklin, and Christoph Moroni. A GFP-based assay for monitoring post-transcriptional regulation of ARE-mRNA turnover. *Molecular BioSystems*, 2(11):561–567, oct 2006. ISSN 1742-2051. doi: 10.1039/B609448A.

[53] Michaela Mickoleit, Torsten U. Banisch, and Erez Raz. Regulation of hub mRNA stability and translation by miR430 and the dead end protein promotes preferential expression in zebrafish primordial germ cells. *Developmental Dynamics*, 240(3):695–703, mar 2011. ISSN 1097-0177. doi: 10.1002/DVDY.22571.

[54] Akihiko Koga, Miho Suzuki, Hidehito Inagaki, Yoshitaka Bessho, and Hiroshi Hori. Transposable element in fish. *Nature*, 383(6595):30, 1996. ISSN 1476-4687. doi: 10.1038/383030a0.

[55] Koichi Kawakami. Transposon tools and methods in zebrafish. *Developmental Dynamics*, 234(2):244–254, oct 2005. ISSN 1058-8388. doi: 10.1002/dvdy.20516.

[56] Koichi Kawakami. Tol2: A versatile gene transfer vector in vertebrates. *Genome Biology*, 8(SUPPL. 1):S7, oct 2007. ISSN 14747596. doi: 10.1186/gb-2007-8-s1-s7.

[57] Darius Balciunas, Kirk J. Wangensteen, Andrew Wilber, Jason Bell, Aron Geurts, Sridhar Sivasubbu, Xin Wang, Perry B. Hackett, David A. Largaespada, R. Scott McIvor, and Stephen C. Ekker. Harnessing a High Cargo-Capacity Transposon for Genetic Applications in Vertebrates. *PLoS Genetics*, 2(11):1715–1724, nov 2006. ISSN 15537390. doi: 10.1371/JOURNAL.PGEN.0020169.

[58] Sarah C.R. Elgin and Gunter Reuter. Position-Effect Variegation, Heterochromatin Formation, and Gene Silencing in Drosophila. *Cold Spring Harbor Perspectives in Biology*, 5(8), aug 2013. ISSN 19430264. doi: 10.1101/CSHPERSPECT.A017780.

[59] Leon Y. Chan, Christopher F. Mugler, Stephanie Heinrich, Pascal Vallotton, and Karsten Weis. Non-invasive measurement of mRNA decay reveals translation initiation as the major determinant of mRNA stability. *eLife*, 7, sep 2018. ISSN 2050084X. doi: 10.7554/ELIFE.32536.

[60] Steven L. Walker, Junko Ariga, Jonathan R. Mathias, Veena Coothankandaswamy, Xiayang Xie, Martin Distel, Reinhard W. Köster, Michael J. Parsons, Kapil N. Bhalla, Meera T. Saxena, and Jeff S. Mumm. Automated reporter quantification in vivo: High-throughput screening method for reporter-based assays in zebrafish. *PLoS ONE*, 7(1), jan 2012. ISSN 19326203. doi: 10.1371/journal.pone.0029916.